NTNU – Trondheim
Norwegian University of
Science and Technology

Pressure Transient Analysis Using Generated Well Test Data from Simulation of Selected Wells in Norne Field

Ilfi Binti Edward Yasin

Petroleum Engineering
Submission date: May 2012
Supervisor: Jon Kleppe, IPT

Norwegian University of Science and Technology
Department of Petroleum Engineering and Applied Geophysics

Master Thesis

Ilfi Binti Edward Yasin

Pressure Transient Analysis Using Generated Well Test Data from Simulation of Selected Wells in Norne Field

Trondheim, May 2012

NTNU
Norwegian University of Science and Technology
Faculty of Engineering and Technology
Department of Petroleum Engineering and Applied Geophysics

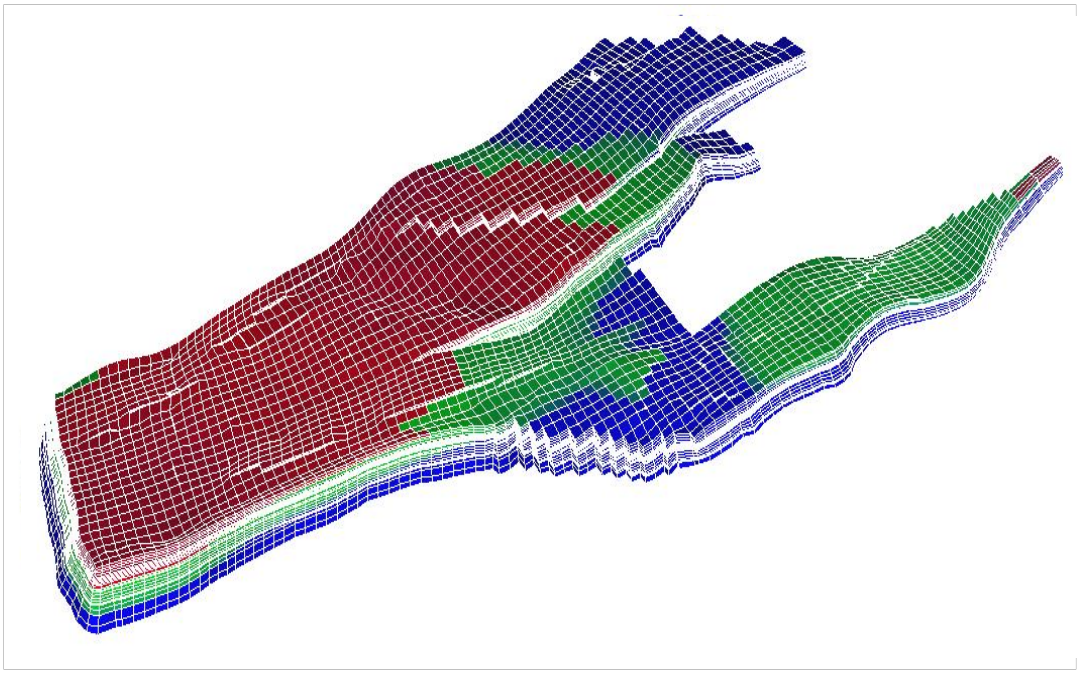

NTNU
Norwegian University of Science and Technology

ABSTRACT

Several types of transient well testing in Norne field are presented in this thesis. One production well from each segment in Norne field was participated in different type of test. The well test data of all cases were generated from reservoir simulation. It allows flexibility in modifying reservoir model condition to understand different behavior of pressure response. The tests were first started by producing the well at a constant rate for 10 days, and then shutting-in the well for at least 24 hours. The importance of reservoir model grid refinement, determination of reservoir communication across the fault, and the complexity of horizontal well test analysis are the three main discussions in this thesis work.

Series of buildup tests at well D-1H in C-Segment were performed to recognize the significance level of Local Grid Refinement (LGR) near the wellbore. There are two sensitivities performed in the reservoir model, extension of LGR area and increase of LGR factor. Based on pressure responses, wider area of LGR affected permeability estimation, while increase of LGR factor impacted the storage capacity calculation. In the next discussions, LGR near the wellbore becomes a standard procedure in generating well test data.

The next type of transient well testing performed in Norne field is interference test. This test was executed at well E-3H as an observation well in E-Segment; while well E-1H and E-2H acted as interfering wells in D- and E-Segments respectively. According to pressure and production trends, it can be ensured both interfering wells are located in different segments. A reservoir communication across segments was identified through pressure drop analysis at well E-3H; hence presence of a major fault between segments is not fully sealed.

Transient well testing in horizontal well gives a special and more complex analysis compare to vertical well analysis. A buildup test was examined at horizontal well E-4AH in G-Segment to determine vertical and horizontal permeability. Two flow regimes existed during the test, early-time radial flow and intermediate-time linear flow. They were discovered from pressure versus time plot and pressure derivative analysis. Interpretation results from both flow regimes show a very low k_v/k_h ratio in the segment around the well.

All data tests were interpreted manually using practical equations after doing comprehensive literature studies. The data were also evaluated quantitatively using F.A.S.T Welltest^{TM} – engineering software of pressure transient analysis from Fekete reservoir engineering software and services. Reservoir properties obtained from pressure transient analysis have similar results with the original data on the reservoir model.

To simplify the study, production rate which was used in build-up and interference tests are only from oil production basis. In addition, no injections in Norne field were included during the tests to have the same comparison in all analysis. As the future work, any other types of tests are strongly recommended, both in single-well and multiple-well testing, also in vertical and horizontal wells.

DEDICATION

This master thesis is dedicated to my beloved parents:

Edward Yasin
and
Hilma Jamain

ACKNOWLEDGEMENT

This work is a master thesis which is compulsory for the final year student. It was written during spring semester in 2012. My deep gratitude goes to my supervisor Professor Jon Kleppe, professor in Reservoir Engineering and Head of The Department of Petroleum Engineering and Applied Geophysics for his help, support, and encouragement during this master thesis work.

Great thanks to Richard Rwechungura, PhD Scholar for providing simulation data of Norne field and giving the opportunity to have discussion with Statoil engineers in Harstad. I also wish to acknowledge Luky Hendraningrat and Mehran Namani, PhD students of Petroleum Engineering for their valuable advice, guidance, and explanation about some technical parts in simulation.

I also wish to say a big thanks to Statoil engineers who has given precious discussion regarding well testing in Norne field during my visit to Harstad.

My sincere thanks also go to Jan Ivar Jensen and Lars Johan Sandvik for their kind support with the IT matter.

Special thanks are extended to many of my fellow friends in IPT for their priceless advice and support during my project work.

Trondheim, May 2012

Ilfi Binti Edward Yasin

TABLE OF CONTENTS

LIST OF FIGURES

LIST OF TABLES

CHAPTER 1
INTRODUCTION

1.1 Background

Transient well testing is one of practical method to characterize reservoir properties or the ability of the formation to produce fluid which has been studied since many years ago. It has advantages compare to other technique in determining reservoir properties. One of them is that well testing covers wider area to interpret, even more it can reach up to its boundary. In addition, many types of test are also available depending on specific parameter to be analyzed.

To understand how it behaves in different reservoir conditions, transient well testing is good to be studied using generated data from reservoir simulation model. The reaction is simply recognized from pressure response by giving certain production or injection rate control. In order to generate sufficient well test data from simulation, the model has to be correctly designed close to its actual condition. One of parameter to be adjusted is the gridding system where Local Grid Refinement (LGR) plays an important role.

Norne field provides a complete reservoir simulation model as a study case. Several segments in the field and numerous numbers of wells are feasible to investigate. Selective wells from each segment can be treated as transient well testing application. Different well directions and completions exist in this field. There are also variety in geological conditions and reservoir properties. These conditions deliver many opportunities to understand many reservoir behavior and characteristics based on pressure transient analysis.

1.2 Objectives

The objectives of this master thesis are listed as follows:

- To evaluate several types of pressure transient analysis in Norne field using generated well test data from simulation. The analysis are conducted both manual calculation and software application.

- To understand the important and significance level of Local Grid Refinement (LGR) application near the wellbore in generating well tests data from simulation.

- To identify reservoir property and communication between wells and/or segments in Norne field based on multiple-well test interpretation.

- To study the characteristic of pressure transient analysis in horizontal well and determine the reservoir property from the analysis.

1.3 Scope of Work

Scopes of work of this master thesis are described below:

- Several wells in Norne field are selected to conduct the well test as a representative of each segment. Different method is applied in different well, so each segment will implement different type of test. Hence, the full field reservoir model is used in generating well test data for the entire work of this thesis.

- The pressure transient analysis is only performed using pressure data during shut-in time because the flow is stable so then it is possible to get sufficient permeability estimation.

- Oil phase is the only fluid that is considered in all analysis as simplification purpose in comparing various cases.

- In any type of transient well testing, no injections in Norne field are included to have the same comparison in all analysis. So, pressure maintenance or enhanced displacement technique is not applied during the tests.

1.4 Report Outline

The rest of this thesis is structured in the following manner:

Chapter 2: **Basic Theory of Transient Well Testing** describes a brief explanation about the types of transient tests and the flow regimes during the test. It is followed by its practical basic interpretations of single-well and multiple-well testing. In addition, basic theory of well testing in horizontal is also described as many horizontal wells were drilled in Norne field.

Chapter 3: **Overview of Norne Field**. This chapter explains the location and geological description of the field including its drainage strategy until 2014. Information about full field reservoir model which will be used in the entire work of this study is briefly described.

Chapter 4: **Effect of Local Grid Refinement (LGR)** gives a detail process of applying refinement near the wellbore in the simulation. Then it will discuss the impact of LGR to the well test data and pressure transient analysis.

Chapter 5: **Interference Test across the Fault** provides series of analysis to characterize the reservoir communication between D-Segment and E-Segment where a major fault is pronounced in between these segments.

Chapter 6: **Transient Well Testing in Horizontal Well**. Interpretations of transient well testing in horizontal well are implemented in this section which recognize the flow regimes and determine the reservoir property.

Chapter 7: **Conclusion and Recommendation** summarizes the analysis performed in this thesis and presents the results achieved. Some recommendations to improve the future work are also listed in this chapter.

CHAPTER 2
BASIC THEORY OF TRANSIENT WELL TESTING

The well test concept is basically sending a signal to the reservoir, then receiving its response from the formation, at the end the permeability can be obtained from its decline. Response which is received at the wellbore is used to evaluate the near wellbore properties. If response from a boundary is reached, so the distance is possible to estimate from the time delay.

The whole process of well test requires specific set-up. The standard well test set-up consists of surface rates, wellhead pressure (WHP), bottom hole pressure (BHP) including bottom hole temperature (BHT), and acquisition interpretation. Transient well testing applies the inverse solution of indirect measurement where input and output are known from the test, while the system is going to predict or estimate from interpretation. The system means well and reservoir characteristics, output represents pressure responses, and input shows a change of rate.

As part of field data, well test data contributes in production analysis model (i.e. well test models, material balance models, and decline curve analysis). Those data are collected become reservoir information that furthermore designed to be a predictive model. This model allows engineers to simulate production forecast and run various scenarios with different production strategies. Finally, economic study and decision making for the field development is conducted by considering many aspects.

Well test can investigates a much larger volume of the reservoir compare to cores and logs. Approximate depth of investigation of coring is only 10 cm and logging is 50 cm, while well testing may reach 50-500 meters of investigation. Its larger area allows the estimations of reservoir permeability, porosity, skin, average pressure, fracture length, heterogeneities, drainage are, shape, open-flow potential, distances to the boundaries, and some others conditions.

2.1 Types of Transient Tests

Certain types of tests are dedicated to specific stage of reservoir discovery, development, and production. In exploration and appraisal wells, Drillstem tests (DSTs) and wireline formation test are normally run. During primary, secondary, and enhanced recovery stages, the conventional transient well tests (i.e. drawdown, buildup, interference, and pulse tests) are run. Step-rate, injectivity, falloff, interference, and pulse tests are executed during secondary and enhanced recovery stages. Some tests are implemented throughout the life of reservoir, such as multilayer and vertical permeability tests [(1)].

Each type of tests has various reservoir properties that can be obtained. Some tests interpret the same properties, but the level of accuracy might be different. For instance, permeability estimated from buildup test gives higher level of accuracy than drawdown test; otherwise skin calculation from buildup test deliver lower accuracy than drawdown test. Table 2.1 lists the types of tests and various data which can be obtained from each test.

Table 2.1 – Reservoir Properties Obtainable from Various Transient Tests [(2)]

Types of Tests	Data Obtained
DSTs	Reservoir behavior Fluid samples Permeability Skin Fracture length Reservoir pressure Reservoir limit Boundaries
Wireline formation tests	Pressure profile Fluid samples Some reservoir properties
Drawdown tests	Reservoir behavior Permeability Skin Fracture length Reservoir limit Boundaries
Buildup tests	Reservoir behavior Permeability Skin Fracture length Reservoir pressure Boundaries

Step-rate tests	Formation parting pressure Permeability Skin
Falloff tests	Mobility in various banks Skin Reservoir pressure Fracture length Location of front Boundaries
Interference and pulse tests	Communication between wells Reservoir type behavior Porosity Interwell permeability Vertical permeability
Layered reservoir tests	Properties of individual layers Horizontal permeability Vertical permeability Skin Average layer pressure Outer boundaries

2.2 Flow Regimes Categories

At different times, fluid flows in the reservoir with different ways generally based on the shape and size of the reservoir. Flow behavior classification is studied in terms of pressure rate of change with respect to time. Three main flow regimes will be described in this sub-chapter; they are steady-state flow, pseudo steady state flow, and transient state flow.

2.2.1 Steady State Flow

In steady state flow, there is no pressure change anywhere with time (Equation 2.1). It occurs during the late time region when the reservoir has gas cap or aquifer support. This condition is also called constant pressure boundary which pressure maintenance might apply in the producing formation. Figure 2.1 shows the log-log plot of pressure drop and pressure derivative versus time of steady state flow regime. Pressure derivative line drops significantly in this type of flow while pressure is constant.

$$\frac{\partial p}{\partial t} = 0 \tag{2.1}$$

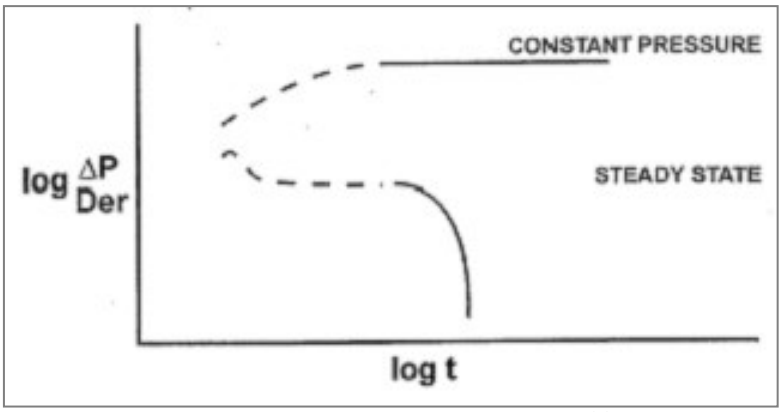

Figure 2.1 – Steady State Flow Plot [3]

2.2.2 Pseudo Steady State Flow

This flow regime also occurs in late-time region, but it forms when there is no flow in the reservoir outer boundaries. No flow boundaries can be caused by the effect of nearby producing or presence of sealing faults. It is a closed system or acts as a tank where a constant rate production results constant pressure drop for each unit of time (Equation 2.2).This flow is also called semi-steady state or depletion state.

$$\frac{\partial p}{\partial t} = constant \tag{2.2}$$

In log-log plot of pressure derivative versus time, this type of flow creates the unit slope (slope equal to one) as illustrated in Figure 2.2. During buildup or falloff tests, pseudo steady state flow is not occurred.

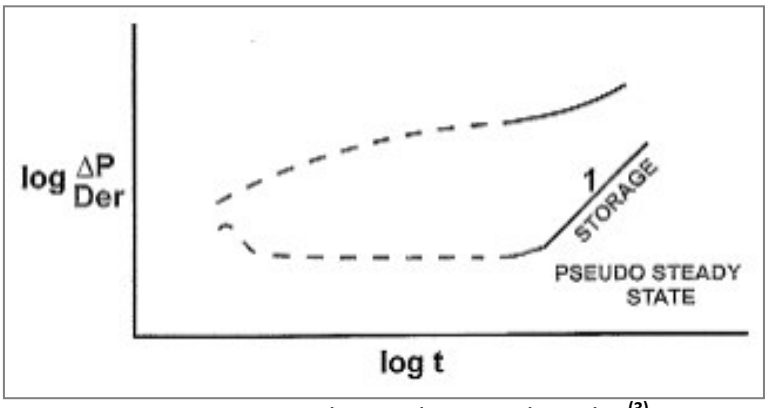

Figure 2.2 – Pseudo Steady State Flow Plot [3]

2.2.3 Transient State Flow

When the pressure/rate changes with time due to well geometry and the reservoir properties (i.e. permeability and heterogeneity), it indicates that transient (unsteady state) flow occurs (Equation 2.3). It is observed before boundary effects are reached or also called infinite acting time period. Higher compressibility of the fluid leads the more pronounced the unsteady state effect of the reservoir fluid [4].

$$\frac{\partial p}{\partial t} = f(x, y, z, t) \tag{2.3}$$

In log-log plot of pressure derivative versus time, this type of flow creates slope equal to zero as illustrated in Figure 2.3. This part of flow usually become a focus on well test interpretation

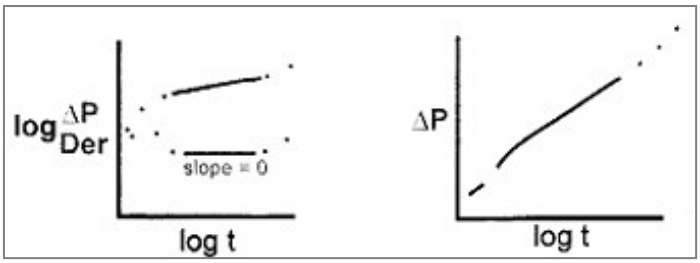

Figure 2.3 – Transient Radial Flow Plot [3]

The typical pressure plot with respect to time for the entire fluid flow behavior in the reservoir is shown in Figure 2.4. Pressure derivative and pressure-time log-log plots with the different time categories are also shown in Figure 2.5. Steady state flow is marked by S.S and pseudo steady state is marked by P.S.S.

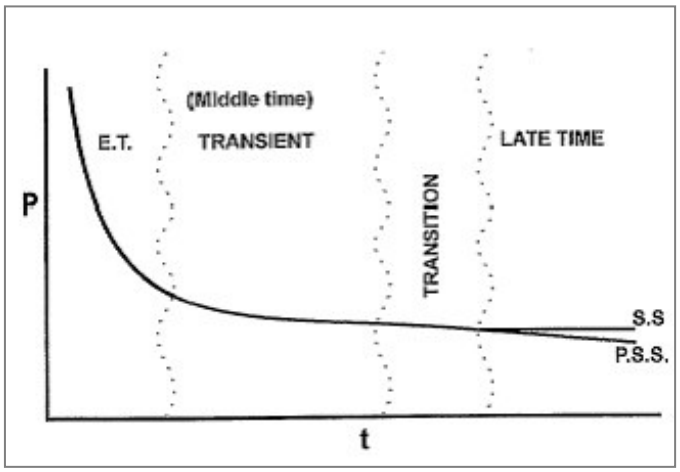

Figure 2.4 – Plot of Pressure vs Time of All Regimes [3]

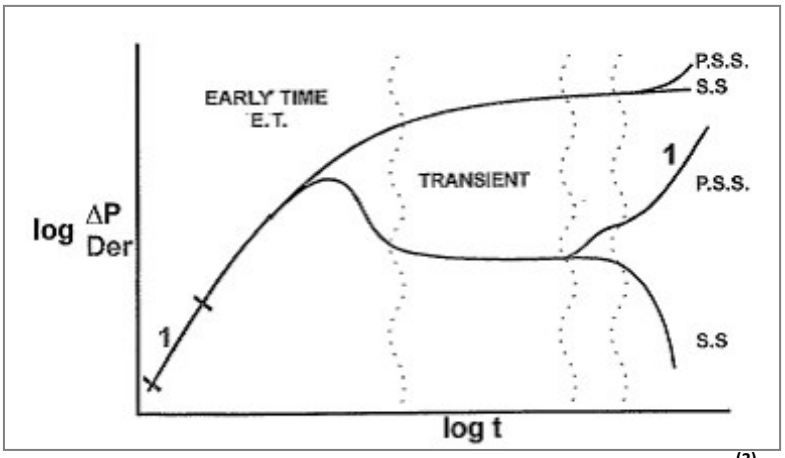

Figure 2.5 – Log-log Plot of Pressure vs Time of All Regimes [3]

For each flow regime categories, there are some specific flow regimes occur. They are listed in Table 2.2 for the vertical wells.

Table 2.2 – Specific Flow Regimes within All Categories [3]

Early Time	Middle Time	Transition	Late Time
Wellbore storage	Radial	Single no-flow boundary	Pseudo-steady state
Linear fracture		Linear channel	Steady state
Bilinear fracture			
Spherical			

2.3 Basic Interpretations

This sub-chapter focuses on basic interpretations of homogenous formation for a simple well test that does not encounter any complications of the reservoir behavior. Rock properties in homogeneous formation do not change anywhere in the reservoir. This ideal condition will not actually occur in real reservoir, but only close enough to be assumed as homogeneous reservoir.

Sequences of fluid regimes during well test is started from wellbore storage, near wellbore conditions, and then ended by late time boundary effects. Transitional characteristic between flow regimes is described from recorded pressure analysis. Using log-log plot, a complete production test can be diagnosed where all flow regimes can be distinguished from one single plot. Therefore, well test interpretations mostly prefer using log-log scale method.

How far the pressure response travels in the reservoir is important to measure, or if specific radius of investigation is already set, then how much time the test is performed can be also estimated. Three types of tests are described in this sub-chapter: drawdown test, buildup test, and interference test. All tests use log-log or

semilog scale as analysis method to recognize different flow regimes and predict several reservoir properties. In the field, buildup is more common than drawdown.

2.3.1 Radius of investigation

Quantitatively and qualitatively, radius of investigation has great significance both in planning and analyzing a well test. It describes the distance (from the tested wellbore) of the transient pressure into the formation if there is an unstable pressure caused by production or closure of a well. It will show that this distance has a correlation with physical properties of the rock and fluid and also depends on the length of time of well testing [5].

There is a time t when the pressure disturbance reaches the distance r_i (radius of investigation). The relationship between t and r_i is given by Equation 2.4.

$$r_i = \left(\frac{kt}{948\,\Phi\mu c_t}\right)^{0.5} \tag{2.4}$$

From equation above, r_i describes a distance at which the pressure disturbance (increase or decrease) simply influences due to production or injection of fluid at constant rate.

The concept of radius of investigation is a guide to plan a well test. For a certain radius of investigation needed, duration of the test is possible to estimate using this concept. Therefore, optimum and effective time will be used which affect the cost of well testing. Effective and optimum cost for well testing is very important since it is considerably expensive, especially for offshore wells.

Equation 2.4 can also be used to estimate the time to achieve stabilized flow which is the time required to reach the reservoir boundary (Equation 2.5). For example, if the well is located in the center of a cylindrical reservoir of limited r_e, by replacing r_i by r_e, then the time required for the stabilized flow is:

$$t_s = 948\frac{\Phi\mu c_t {r_e}^2}{k} \tag{2.5}$$

To use the concept of radius of investigation, it should be fully considered that this concept will give precise result if only the investigated formations have homogeneous behavior, isotropic, and cylindrical. The existence of heterogeneity of a reservoir will reduce the accuracy of above equations.

2.3.2 Drawdown

Drawdown test is ideally performed when the pressure is equalized throughout the formation. This condition can be reached by shutting-in the well prior to drawdown test or after having several days of workover job. Performing a drawdown test at new wells becomes a good recommendation because the reservoir still has a uniform pressure.

Basically, this test measures bottom hole pressure during a period of constant production rate. The equipment is first set into the well, and then begins a constant flow rate. The consideration for having this test is simply when there are some uncertainties in buildup interpretations. Therefore, analysis from drawdown test can be used for comparative analysis [6].

There are three different methods to analyze pressure drawdown data according to its flow regimes during a test. Transient method is used for pressure data which is at a time value of

$$t = 0.1\frac{\Phi\mu c{r_e}^2}{k} \tag{2.6}$$

and semi-steady state method (reservoir limit test) is at later time of the test, while a late transient method exists between these two flow regimes. This section will only present transient drawdown analysis method because generally all drawdown tests have this type of flow.

The simplification of pressure behavior of a well in an infinite reservoir during a constant flow rate is given by

$$p_{wf} = p_i - 162.6\frac{q\mu B}{kh}\left[log\frac{kt}{\Phi\mu c{r_w}^2} - 3.23 + 0.87s\right] \tag{2.7}$$

Figure 2.6 illustrates a schematic transient drawdown analysis plot. A semilog plot of bottom hole pressure p_{wf} versus log time t should be linear with a slope m. Product of kh can be obtained from

$$kh = 162.6\frac{q\mu B}{m} \tag{2.8}$$

If the slope has been calculated, then the skin factor can be estimated from the intercept at time equals to one or log t equals to zero as indicated on Figure 2.6. By rearranging Equation 2.7, the skin factor can be obtained as follow

$$s = 1.15\left[\frac{p_i - p_{1\,hr}}{m} - log\frac{k}{\Phi\mu c r_w{}^2} + 3.23\right] \tag{2.9}$$

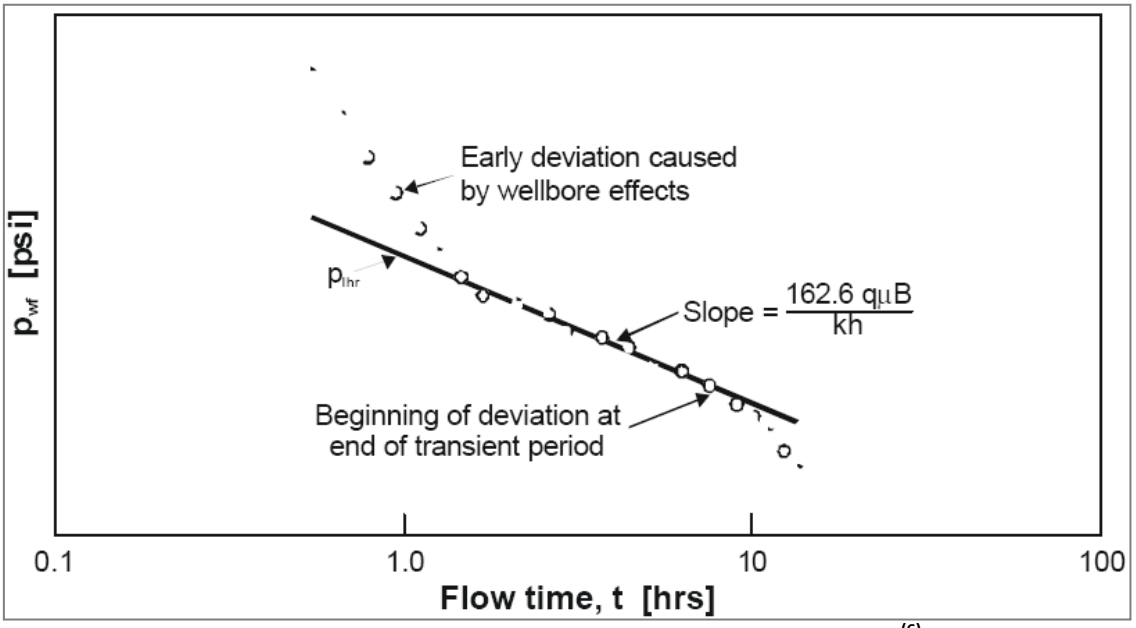

Figure 2.6 – Schematic Transient Drawdown Analysis Plot [6]

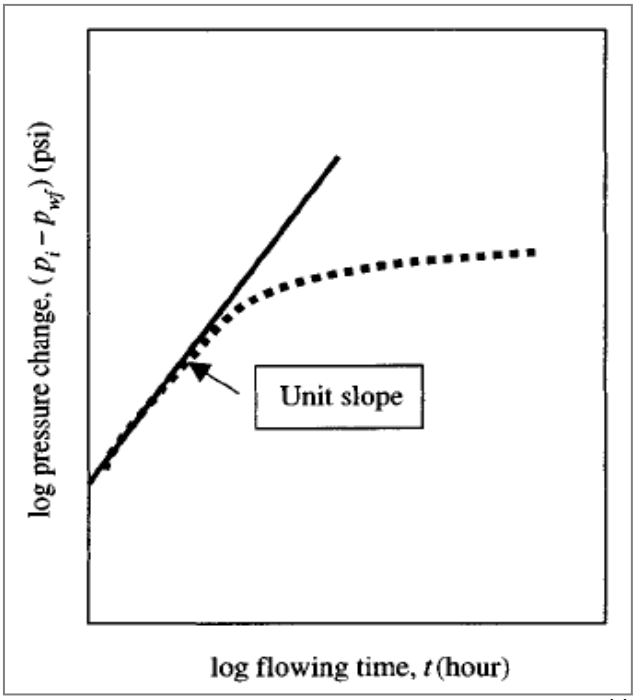

Figure 2.7 – Log-log Pressure Drawdown Data Plot [4]

The nonlinear part of the plot shown in Figure 2.6 exists in a short duration due to unstable flow condition in the tubing string, skin effect, and annulus unloading [6]. From the plot, duration of this period is easily recognized. This nonlinear line can be analyzed using log-log plot of [log (p_i-p_{wf})] versus log t (Figure 2.7) to estimate the wellbore storage coefficient C (bbl/psi). Result of the compressible nature of the fluids in the wellbore is called wellbore storage [7] [8]. When the slope of this line is equal to one, then it means that wellbore storage occurs. Formula used in this estimation is given by Equation 2.10 where Δt and Δp are read from a point on log-log unit slope straight-line.

$$C = \frac{qB}{24}\frac{\Delta t}{\Delta p} \tag{2.10}$$

2.3.3 Buildup

A constant production rate q for a period of time t is usually conducted prior to buildup test. Producing a well at constant rate represents the drawdown part of the well history. Buildup test is started right after t_p (which is representing the duration of production) with zero production by shutting-in the well at the wellhead. Measurement of bottom hole pressure is normally performed since the beginning of drawdown part until the end of buildup test.

A method to analyze the pressure response of buildup test is using Horner method (1951). It is a semilog plot of shut-in pressure p_{ws} versus horner time $(tp+\Delta t)/\Delta t$ as illustrated in Figure 2.8. This plot creates a straight-line which represents the transient flow during the middle-time of the test. Different behavior regions during buildup test are shown in Figure 2.9. Middle-time region indicates that the pressure transient has spread away from the wellbore into the formation [4]. Slope of the straight-line m is a tool to predict reservoir permeability by using below formula

$$kh = 162.6\frac{q\mu B}{m} \tag{2.11}$$

Above formula is based on an equation of pressure response during the buildup period which assumes an infinite-acting reservoir, no boundary effect, homogeneous, slightly compressible, and single-phase fluid flow. The equation is

$$p_{ws} = p_i - 162.6\frac{q\mu B}{kh} log\frac{t_p + \Delta t}{\Delta t} \tag{2.12}$$

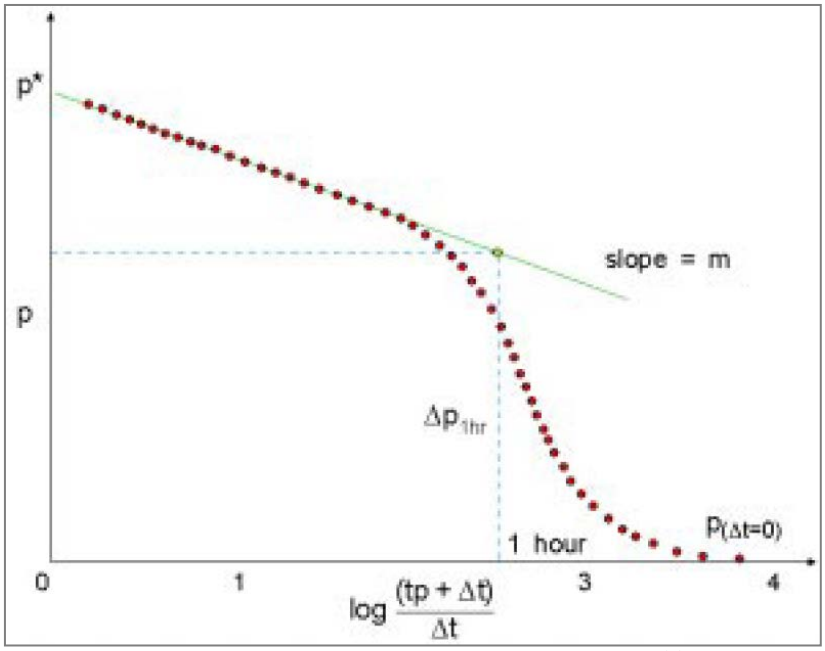

Figure 2.8 – Horner Plot of Buildup Analysis [9]

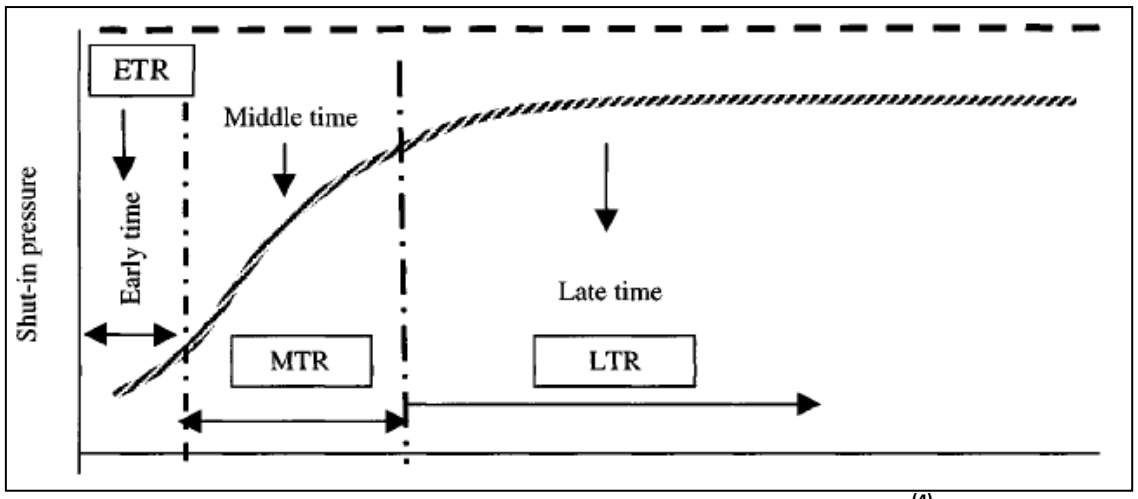

Figure 2.9 – Behavior of the Static Pressure on Shut-in Well [4]

The nonlinear part of the curve on Figure 2.8 indicates the effect of afterflow or wellbore storage. Skin factor may also cause the early-time deviation which can be positive or negative. Positive skin can be formed due to wellbore damage, otherwise a negative skin indicates stimulation (fracturing, acidizing, etc). This shape is formed at the beginning of the curve which means that a pressure transient is spreading around the formation nearest the wellbore [4].

Equation 2.13 is a simplification formula to estimate skin factor, where the value of *m* should be positive. Well flowing pressure p_{wf} is the last pressure before the well shut-in.

$$s = 1.151\left[\frac{p_{1\,hr} - p_{wf(\Delta t=0)}}{m} - log\left(\frac{k}{\Phi\mu c {r_w}^2}\right) + 3.23\right] \quad (2.13)$$

The duration of wellbore storage effect in a buildup test strongly depend on the size and configuration of a wellbore. Using the same technique in drawdown analysis, this effect can be clearly seen from log-log plot of $\Delta p = (p_{ws}-p_{wf})$ versus Δt where a unit slope from initial data is created. From the unit slope, wellbore storage coefficient C is able to estimate using Equation 2.10 that has been mentioned earlier. Wellbore storage is usually formed at the first 1.5 log cycle.

2.3.4 Interference Test

Interference test is part of multiple-well test which involves more than one well during the test. It is the oldest type of multiple-well testing and the first analysis method was reported in 1935. Predicting interwell reservoir properties and interpreting communication between wells are the basic purposes of this test. As a multiple-well test, interference test can be applied not only between neighboring wells, but also between different sets of perforations in one wellbore. Neighboring wells test is used to determine areal reservoir properties or horizontal properties, while different perforation sets test is used to determine vertical properties [(1)].

Product of mobility-thickness kh/μ and porosity-compressibility-thickness $\Phi c_t h$ are the two values that can be estimated from interference test in homogenous isotropic reservoirs. In addition, permeability in different axes can also be determined in a proper designed multiple-well test of homogenous anisotropic reservoirs. To recognize the heterogeneity of a reservoir, then multiple-well test is more sensitive rather than single-well test [(10)].

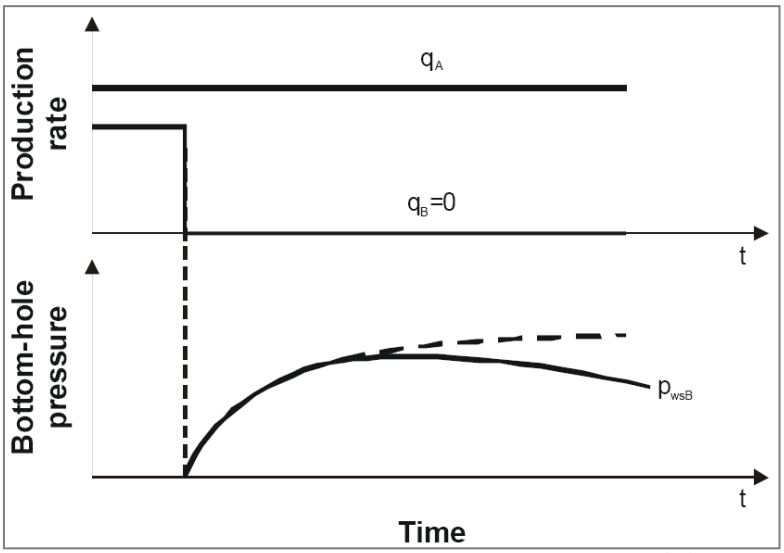

Figure 2.10 – Pressure Data of Interference Test [(11)]

A standard process of an interference test is mainly measuring a pressure drop at an observation well caused by production or injection at an active well in a reservoir. Typical pressure data of interference test is shown in Figure 2.10. Very long shut-in time at observation well can be required to recognize the pressure drop which is affected by the value of *Φμc/k* between the wells. The equation to calculate pressure drop at observation well due to production at offsetting wells is shown below

$$\Delta p = \frac{-m}{2.303}\left[\sum_{i=1}^{NW}\frac{q_j}{q}\left\{Ei\left(\frac{-\Phi\mu c a_j{}^2}{0.00105k\left(t_j+\Delta t_j\right)}\right)-Ei\left(\frac{-\Phi\mu c a_j{}^2}{0.00105kt_j}\right)\right\}\right] \qquad (2.14)$$

where

q = production rate of observation well prior to shut-in
q_j = production rate of Well j
t_j = producing time of Well j prior to shut-in of the observation well
Δt_j = producing time interval of Well j after shut-in of the observation well
NW = number of interfering wells
a_j = distance of Well j to the observation well
Φμc/k = reservoir properties

Permeability data in Equation 2.14 can be estimated using type curve matching method applied for infinite acting reservoirs. This analysis method was the most common technique for interference test in the 1970s and 1980s because of the inadequacy of computers and software. Plot of pressure drop data versus time in an observation well is going to be matched in the type curve of exponential integral solution using the same log-log scale. This type curve is shown in Figure 2.11 plotted as p_D versus $t_D/r_D{}^2$. These three dimensionless forms are generated from below equations:

$$p_D = \frac{\left(p_i - p_{wf(t)}\right)kh}{141.2\ q\mu B} \qquad (2.15)$$

$$t_D = 0.00026372\frac{kt}{\Phi\mu c_t r_w{}^2} \qquad (2.16)$$

$$r_D = \frac{r}{r_w} \qquad (2.17)$$

The point obtained from type curve matching is used to calculate permeability and product of porosity-total compressibility by rearranging the three equations above become

$$k = 141.2\frac{q\mu B}{h}\frac{(p_D)_{MP}}{(\Delta p)_{MP}} \tag{2.18}$$

$$\Phi c_t = \left[0.0002637\frac{k}{\mu r^2}\right]\frac{(\Delta t)_{MP}}{(t_D/{r_D}^2)_{MP}} \tag{2.19}$$

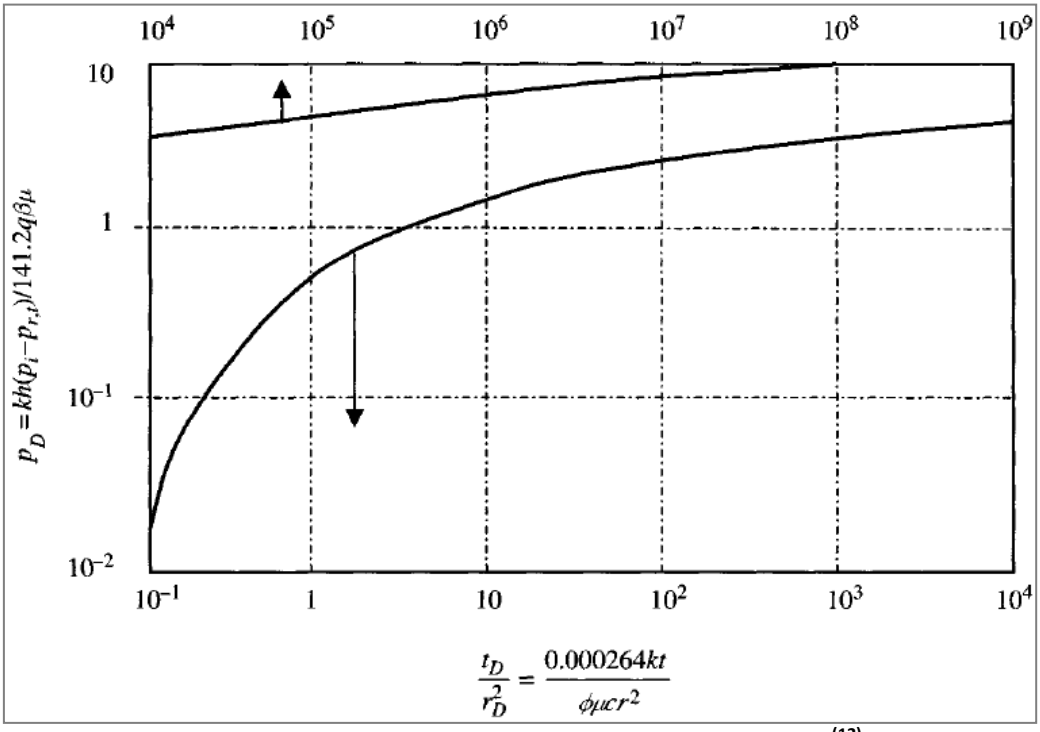

Figure 2.11 – Exponential Integral Solution Type Curve [12]

2.4 Well Testing in Horizontal Wells

As a technique to improve production performance, horizontal wells deliver a very high desirable production enhancement. Wider well surface area allows more withdrawal from the formation. It also prevents early coning compare to partial penetration in vertical wells.

Compare to vertical oil wells, transient well testing in horizontal wells demonstrate more complex behaviors and analysis in characterizing reservoir properties. Various designs of horizontal wells lead this complexity where most of the wells are not perfectly horizontal parallel to bedding plane. Location of the wells can be in the middle of reservoir thickness, close to bottom boundary, or close to top boundary which is also counted to flow behaviors difference. In many cases it makes the interpretation more difficult. Three important parameters that affect transient well testing in horizontal wells are well length, formation thickness, and the ratio of vertical/horizontal permeability.

2.4.1 Transient Flow Regimes

For horizontal wells cases, it can be identified 3 types of transient flow regimes during infinite-acting period, they are:

- ***Early-Time Radial Flow (ERF)***

This flow regime is also called *radial flow in the vertical plane*. It is identical with infinite-acting flow of a vertical well that penetrates all the reservoir thickness. As illustrated in Figure 2.12, the pressure transient is moving radially from the wellbore and has not influenced by boundaries effect [4]. At the time boundaries impact reaches the wellbore, then ERF period ends.

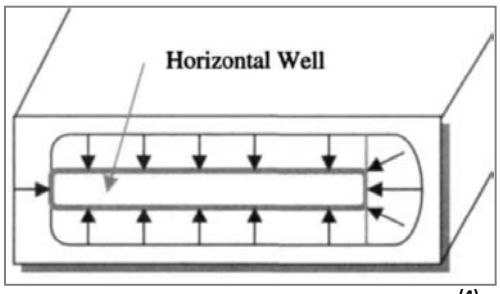

Figure 2.12 – Early-Time Radial Flow [4]

- ***Intermediate-Time Linear Flow (ILF)***

In this period, fluid flows in y-direction and identical to early-time linear-flow regime of a vertically fractured well with the same horizontal penetration [1]. The length of horizontal well is generally longer compared to formation thickness. High vertical permeability also affects this flow regime. When flow in x-direction start to contribute, then ILF period ends. Figure 2.13 shows illustration of this flow regime.

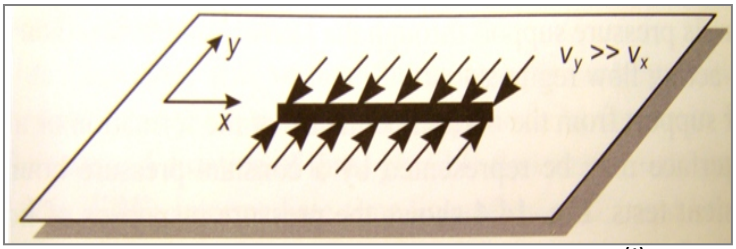

Figure 2.13 – Intermediate-Time Linear Flow [1]

- ***Late-Time Radial Flow (LRF)***

Late-time radial flow exists when length of horizontal well is shorter enough than formation thickness and flow across the tips of the well becomes considerable [4] [1].

This flow regime is also called *horizontal radial flow regime*. Similar flow behavior also occurs in a vertically fractured well. It is also known as pseudo-radial flow that establish at late times. This period ends when lateral boundaries affect the fluid flow. As shown in Figure 2.14, the fluid flow converges from all directions towards the wellbore.

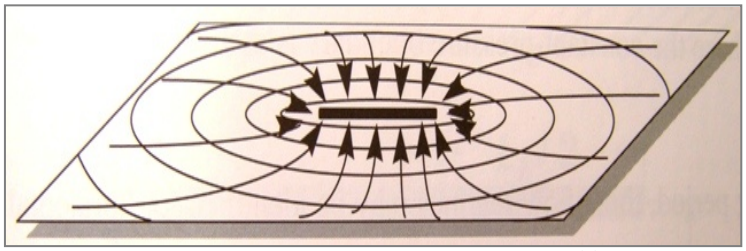

Figure 2.14 – Late-Time Radial Flow [1]

When the lateral boundaries give considerable effect to the flow, it means that boundary-dominated flow has just started. For closed reservoir, this regime is also known as late-time linear flow where the length of horizontal well is more than half of the reservoir thickness. If it is less than half of formation thickness, then it will have the same behavior as those for vertical and vertically-fractured wells [1].

2.4.2 Pressure Response Analysis

Each flow regimes has certain computation to determine several well parameters or reservoir parameters. Both drawdown and buildup tests are discussed in this section. The same as implemented in vertical well, straight-line analysis is also applied in horizontal well testing.

2.4.2.1 Drawdown Test

- **ERF Analysis**

By creating a semilog plot of wellbore pressure p_{wf} or $(p_i\text{-}p_{wf})$ versus *log t*, then a slope m_1 of the straight-line is given by

$$m_1 = 162.6\frac{q\mu B}{\sqrt{k_v k_y}L} \tag{2.20}$$

By rearranging above formula, then permeability around wellbore can be calculated as

$$\sqrt{k_v k_y} = 162.6\frac{q\mu B}{m_1 L} \tag{2.21}$$

Then skin factor *s* can be calculated using below formula

$$s = 1.151\left[\frac{p_i - p_{1\,hr}}{m_1} - log\left(\frac{\sqrt{k_v k_y}}{\Phi\mu c_t {r_w}^2} + 3.23\right)\right] \quad (2.22)$$

Pressure at time equal to 1 hour p_{1hr} is the pressure obtained by extrapolating the straight-line to t = 1 hr. Skin factor in this formula is formed during drilling and completion, known as mechanical skin damage. Oil production rate q means the oil rate during drawdown test which is maintained at a constant rate. The horizontal well has an effective length that is symbolized by L; and well radius is r_w. More properties affected this analysis are porosity Φ, oil viscosity μ, and total compressibility c_t. All of them were determined earlier from core analysis and fluid laboratory experiment.

- **ILF Analysis**

Different plot is made in this flow regime; slope m_2 will be captured from Cartesian plot of p_{wf} or $(p_i\text{-}p_{wf})$ versus $\sqrt{t}$. It is given by below formula

$$m_2 = 8.128\frac{qB}{Lh}\sqrt{\frac{\mu}{\Phi c_t k_y}} \quad (2.23)$$

Rearranged above formula produces multiple of permeability k_y and square of well length L^2

$$L_2 k_y = \left(8.128\frac{qB}{hm_2}\right)^2 \frac{\mu}{\Phi c_t} \quad (2.24)$$

Then, at $\sqrt{t}$ equal to zero of straight-line extrapolation, the pressure response is

$$\Delta p|_{t=0} = 141.2\frac{q\mu B}{L\sqrt{k_y k_v}}(s_z + s) \quad (2.25)$$

By combining the last two formulas above, $\sqrt{k_v}$ can be obtained, hence skin factor is calculated as

$$s = \frac{0.058}{h}\sqrt{\frac{k_v}{\Phi\mu c_t}}\left(\frac{p_i - p_{wf}(0h)}{m_2}\right) - s_z \quad (2.26)$$

Introducing

$$s_z = ln\left(\frac{h}{r_w}\right) + 0.25ln\left(\frac{k_y}{k_v}\right) - ln\left(\sin 180^\circ\left(\frac{z_w}{h}\right)\right) - 1.838 \quad (2.27)$$

where z_w is vertical location of well (ft) and h is reservoir height (ft). Pseudo-skin factor s_z is formed due to partial penetration in z-direction.

- **LRF Analysis**

Semilog plot of wellbore pressure p_{wf} or $(p_i\text{-}p_{wf})$ versus *log t* generates a straight-line with slope m_3 given by following formula

$$m_3 = 162.6\frac{q\mu B}{\sqrt{k_x k_y}h} \quad (2.28)$$

Horizontal permeability k_h is retrieved by rearranging the above formula

$$k_h = \sqrt{k_x k_y} = 162.6\frac{q\mu B}{m_3 h} \quad (2.29)$$

Finally, skin factor is calculated as follow

$$s = 1.151\frac{L}{h}\sqrt{\frac{k_v}{k_x}}\left[\frac{p_i - p_{1\,hr}}{m_3} - log\left(\frac{k_x}{\Phi\mu c_t L^2}\right) + 2.023\right] - s_z \quad (2.30)$$

By extrapolating the straight-line to time equal to 1 hour, then p_{1hr} is known. Pseudo-skin factor s_z is also determined using Equation 2.27.

2.4.2.2 Buildup Test

Prior to shut-in, the well is normally producing for much longer time compare to shut-in period. Hence the horner time $log\ (t_p+\Delta t)/\Delta t$ can be written as $(log\ t_p - log\ \Delta t)$, so then the resulting data is independent of production history.

- **ERF Analysis**

As general method for buildup test, horner plot also conduct in horizontal well testing analysis. From the semilog plot of pressure drop Δp versus $log\ (tp+\Delta t)/\Delta t$, then a straight-line will be exhibited with slope m_{1r} as presented in formula below

$$m_{1r} = 162.6\frac{q\mu B}{\sqrt{k_v k_y}L} \tag{2.31}$$

Extrapolation of this straight-line cannot be used for estimating the pressure at infinite shut-in time p^*. By rearranging the formula, permeability around wellbore in vertical plane is calculated by

$$k_v k_y = \left(162.6\frac{q\mu B}{m_{1r}L}\right)^2 \tag{2.32}$$

Determine pressure at time equal 1 hour p_{1hr} from the extrapolation of the straight-line, then the skin factor can be estimated by

$$s = 1.151\left[\frac{p_{1\,hr} - p_{wf}}{m_{1r}} - log\left(\frac{k_v k_y}{\Phi\mu c_t {r_w}^2}\right) + 3.23\right] \tag{2.33}$$

- **ILF Analysis**

Cartesian plot of Δp versus $\sqrt{t}$ is generated in this flow regime. Slope m_{1l} of the straight-line is given by below formula

$$m_{1l} = 8.128\frac{qB}{h\sqrt{k_v k_y}} \tag{2.34}$$

By rearranging above formula, then permeability around wellbore can be calculated as

$$k_v k_y = \left(8.128\frac{qB}{m_{1l}h}\right)^2 \tag{2.35}$$

From the same plot and slope, permeability in y-direction can be calculated using below formula [3]

$$\sqrt{k_y} = 8.128\frac{q\mu B}{mhL\sqrt{\Phi\mu c_t}} \tag{2.36}$$

Then skin factor s can be calculated using below formula

$$s = \frac{0.058}{h}\sqrt{\frac{k_v}{\Phi\mu c_t}}\left[\frac{p_{1h} - p_{wf}}{m_{1l}}\right] - s_z \tag{2.37}$$

- **LRF Analysis**

From the semilog plot of wellbore pressure p_{wf} versus *log (tp+Δt)/Δt*, then a straight-line will be created with slope m_{2r} as presented in formula below

$$m_{2r} = 162.6\frac{q\mu B}{h\sqrt{k_v k_y}} \tag{2.38}$$

If this flow regime presents, the extrapolation of the straight can be used to predict the pressure at infinite shut-in time *p**. Finally, skin factor s_m is calculated as follow

$$s_m = 1.151\frac{L}{h}\sqrt{\frac{k_v}{k_x}}\left[\frac{p_{1\,hr} - p_{wf}}{m_{2r}} - log\left(\frac{k_v}{\Phi\mu c_t L^2}\right) + 2.023\right] - s_z \tag{2.39}$$

2.4.3 Pressure Derivative Behavior

By combining the pressure response analysis (plot of pressure versus time) with pressure derivative log-log plot, pressure transient analysis will be easier to interpret. Different flow regimes are more obvious to detect, hence the identification of some parameters also receive higher level of confident. To specify the starting time of pseudo-steady-state flow, pressure derivative gives a distinct behavior on it by showing a slope of 2π from p_{WD} versus t_{DA} curve. Horizontal well response and normalized pressure derivative is presented in Figure 2.15. This curve contains the data of dimensionless pressure p_{WD} versus dimensionless time t_D. Dimensionless time t_D and t_{DA} are given by

$$t_D = 0.000264\frac{kt}{\Phi\mu c_t {r_w}^2} \tag{2.40}$$

and

$$t_{DA} = 0.000264\frac{kt}{\Phi\mu c_t A} \tag{2.41}$$

Large wellbore storage is frequently resulted in horizontal well testing that impacts the first radial flow difficult to interpret. In horizontal well, the last flow regimes not always presented in pressure derivative analysis with a standard test period [13]. This kind of complexity in horizontal well becomes a challenge during interpretation of both pressure-time data and pressure derivative behavior. Figure 2.16 shows plot of dimensionless pressure and derivative versus dimensionless time. The first stabilization represents the initial radial flow, while the last derivative stabilization indicates pseudo-radial flow.

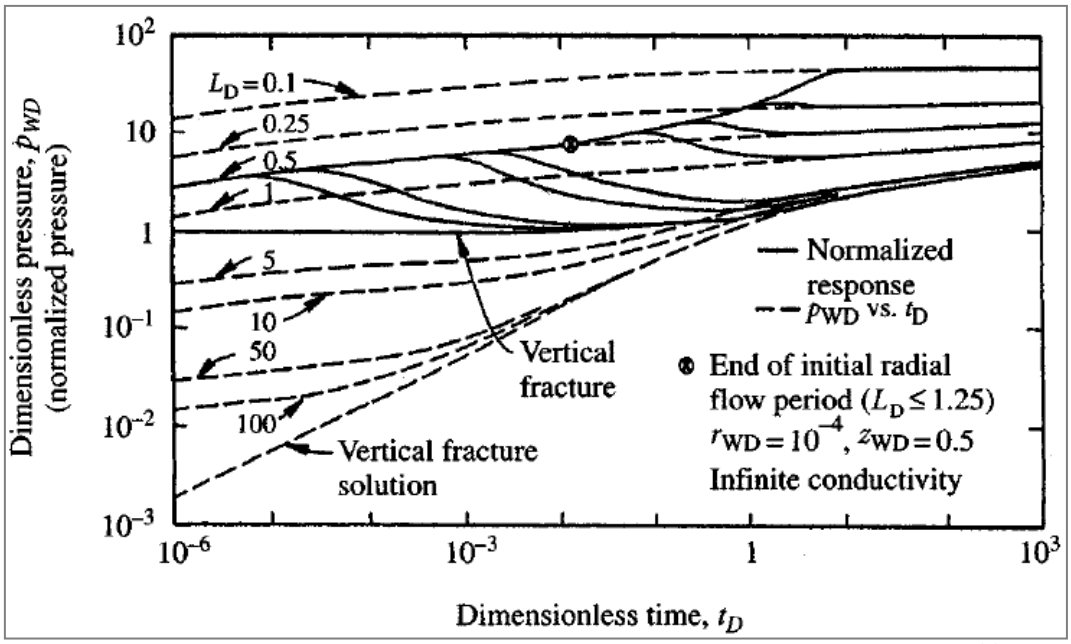

Figure 2.15 – Horizontal Well Response and Normalized Pressure Derivative [4]

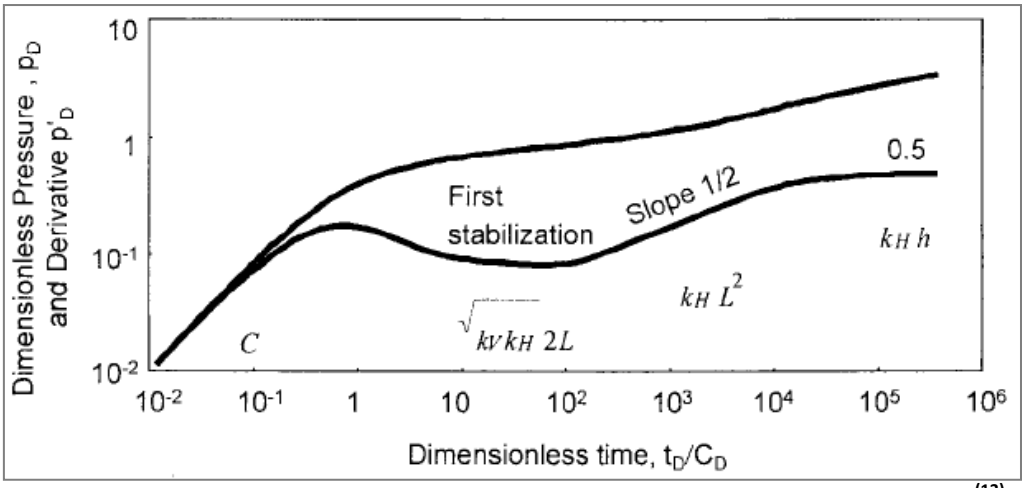

Figure 2.16 – Dimensionless Pressure and Derivative versus Dimensionless Time [13]

Complete identification of flow regimes from derivative response can be followed by determining some parameters from each of them. Unit slope straight-line from early time period and final stabilization are used to estimate permeability-thickness product $k_H h$ and wellbore storage coefficient C after matching the time and pressure. The effective well half-length L is predicted from intermediate time linear flow regime by matching the data on the half unit slope straight-line, whereas the first derivative stabilization defines permeability ratio (anisotropy) k_V/k_H and mechanical skin S_w. If wellbore storage is too dominant in vertical radial flow, then permeability ratio k_V/k_H is not able to estimate. The total skin from late time data will not be accurate. When the well testing data does not reach the final derivative stabilization, horizontal permeability k_H and total skin S_w are not reliable, while half unit slope straight-line is able to predict product of horizontal permeability and square of effective well length $k_H L^2$ [13].

CHAPTER 3
OVERVIEW OF NORNE FIELD

Norne field is located in the Southern part of the Nordland II are, positioned at blocks 6608/10 and 6508/10 [14]. It is an oil and gas field on the Norwegian continental shelf, 80 km north of the Heidrun field. Sea depth around the field is about 380 meter, hence it requires production and storage vessel which is transported by Statoil ASA and its partners from Harstad. The field was first discovered in December 1991, started drilling operation in August 1996, and production began in November 1997 [15] [16]. Figure 3.1 shows the location map of Norne field that located 200 km west of Brønnøysund or Sandnessjøen.

There are two oil compartments in Norne field; they are Norne Main Structure and Norne-East Segment. Norne Main Structure is an area of Norne C-, D-, and E-segments, where the most of oil in place is accumulated (97%). This structure is relatively flat and filled by gas (approximately 25 meter gas column) in Garn formation which has Gas-Oil Contact (GOC) along the Not Formation clay stone. Ile and Tofte formations contain roughly 80% of oil or around 110 meter oil column (based on well 6608/10-2). Norne G-segment was the later discovery as part of Norne-East Segment. No gas cap found in this segment. Those segments are shown in Figure 3.2.

The recoverable reserve of Norne field is estimated around 90.8 x 10^6 Sm^3 of oil and 11.8 x 10^9 Sm^3 of gas. Oil production reached approximately 94.9% of recoverable reserves or in total 86.2 x 10^6 Sm^3 up to 31 December 2011 [17]. As of year 2010, there are total 50 wells that have been drilled in Norne field, include 33 producers, 10 water injectors, and 7 observation wells. Active wells only consist of 16 producers, and 8 water injectors.

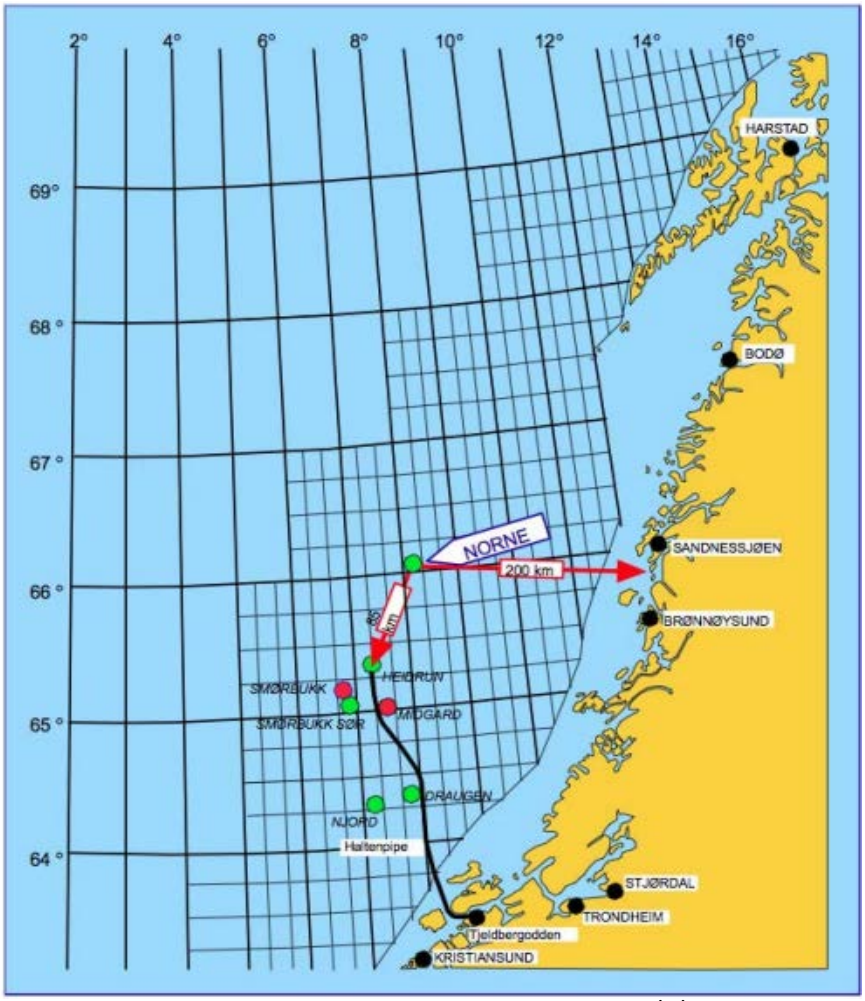

Figure 3.1 – Location Map of Norne Field [16]

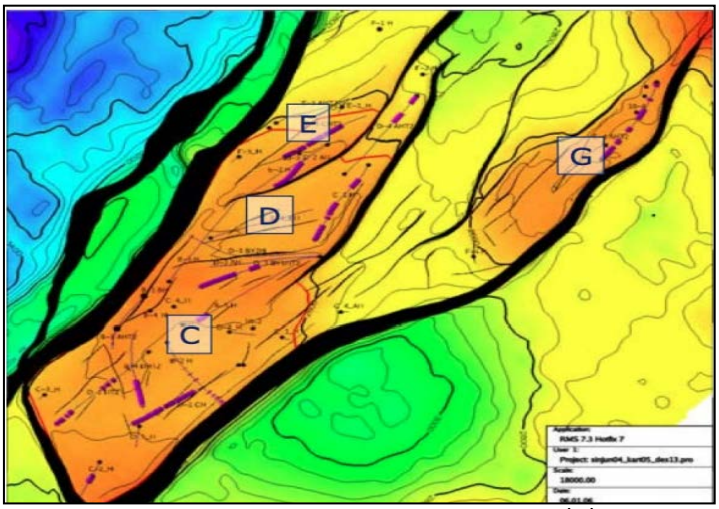

Figure 3.2 – Segments in Norne Field [16]

3.1 Geological Information

Reservoir in Norne field is formed as sandstones located in the Lower to Middle Jurassic sandstones based on stratigraphical study. It is dominated by fine-grained and well to very well-sorted which is existed at depth of 2500-2700 meter. As a diagenetic process, mechanical compaction reduces the reservoir quality; and currently it has 25-30% of porosity and 20 – 2500 mD of permeability.

The petroleum system can be described as follow:

- **Reservoir**. It is divided into four different formations from top to bottom: Garn, Ile, Tofte, and Tilje.
- **Source rock**. There are two source rocks predicted for this reservoir. The first one is Spekk formation from Late Jurassic, and the other one is coal bedded Åre formation from Early Jurassic
- **Cap rock**. To trap the oil and gas in place or seal the reservoir, a cap rock is required. The cap rock in this system is believed from Melke formation in Middle Jurassic series
- **Sealing layer**. Not formation lies between Ile formation and Garn formation, as a sealing layer to prevent communication between these two formations. It is located in Aalenian stage of Middle Jurassic.

The stratigraphical log of all formations mentioned above can be seen in Figure 3.3. Total thickness from Åre to Top Garn formation is 120 meter in northern part, or 260 meter in southern part. The difference between northern and southern part of the reservoir is due to erosion in Ile and Tilje formation in the north [18]. Figure 3.4 illustrates cross-section through reservoir zone isochores.

Brief description of all formations in Norne field is presented in Table 3.1. The information is including thickness of the formations, sediment deposited, deposition age, and depositional environment.

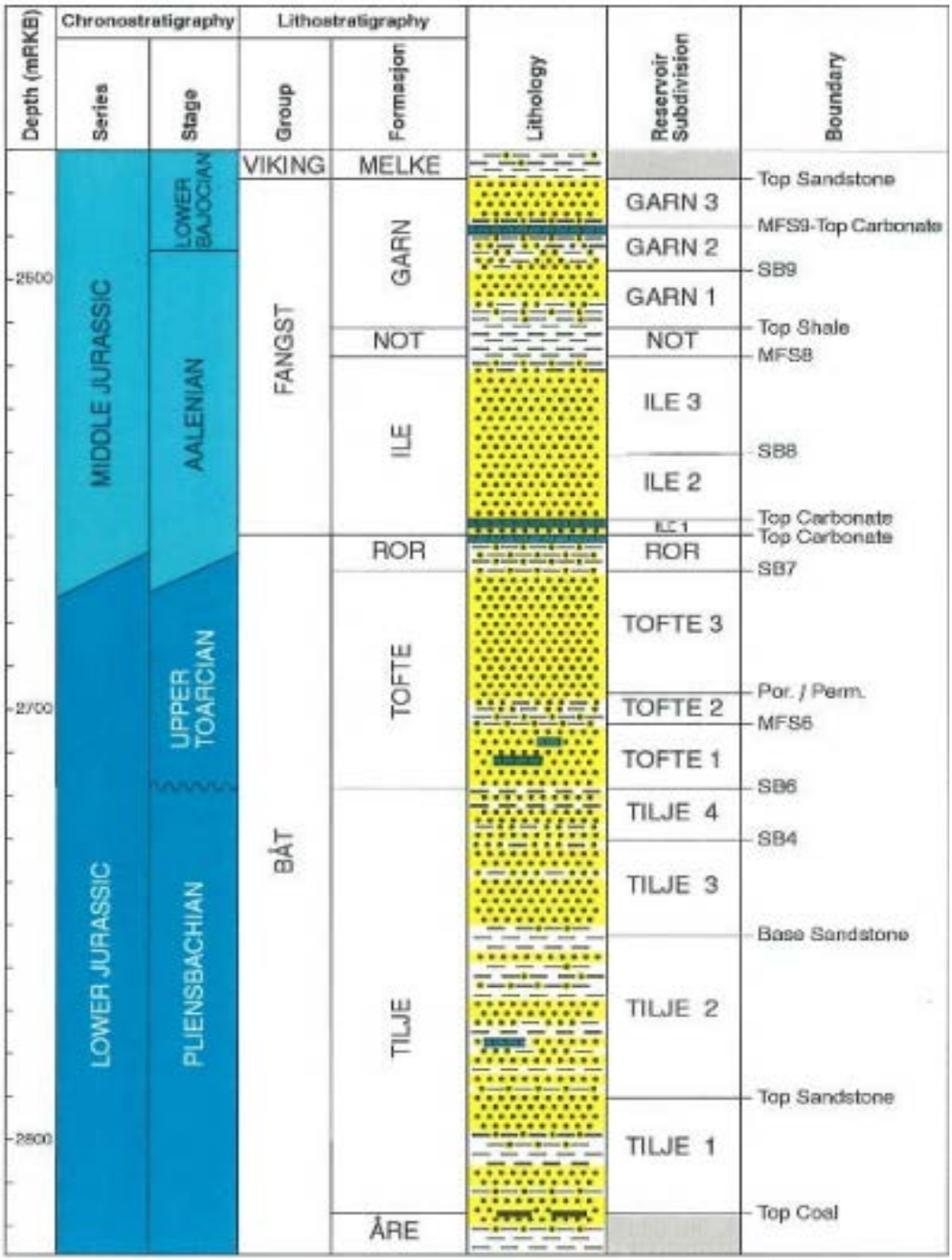

Figure 3.3 – Stratigraphical Sub-division of Norne Reservoir [19]

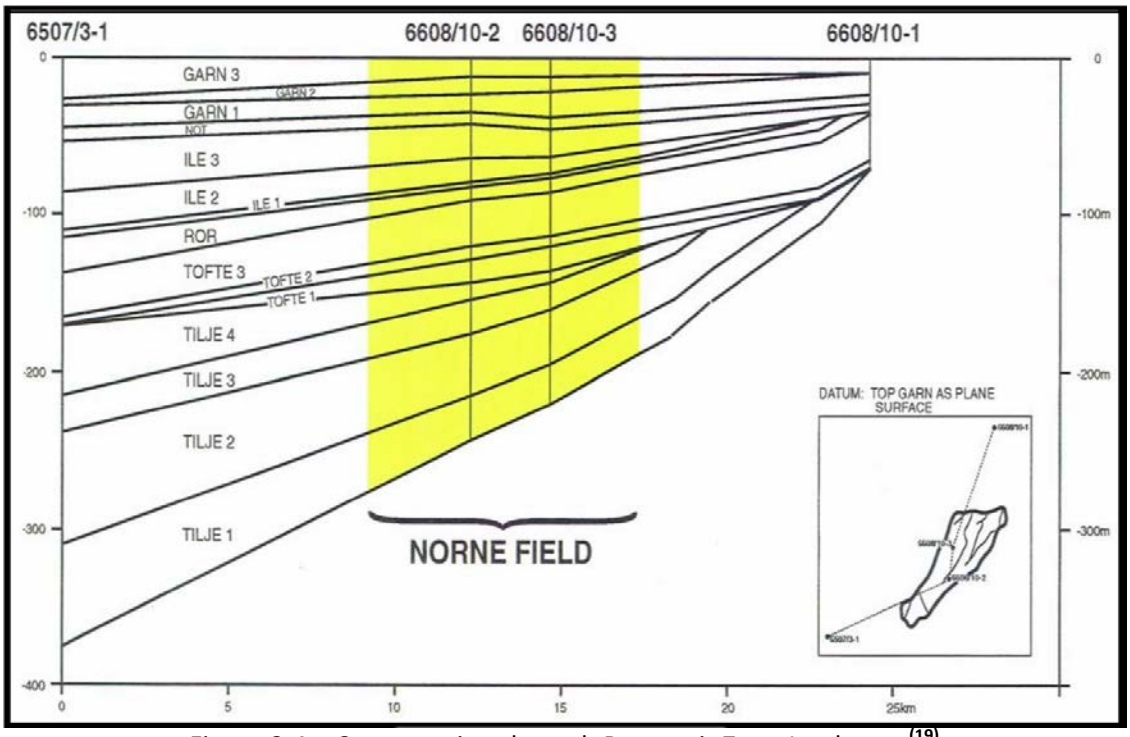

Figure 3.4 – Cross-section through Reservoir Zone Isochores [19]

Table 3.1 – Description of Formations in Norne Field

Formation	Thickness	Sediment Deposited	Deposition Age	Depositional Environment
Åre	200 - 800 meters	Channel sandstones, interbedded with mudstones, shales, and coals	Hettangian to Early Pliensbachian	Alluvial to delta plain
Tilje		Sand with some clay and conglomerates		Marginal marine
Tofte	50 meters	Shales, whilst sand	Late Toarcian	Marine from foreshore to offshore
Ror	8.5 meters	Very fine grained/shaly unit	Time equivalent with the Tofte Formation	Lower shoreface, with low sediment supply
Ile	32 - 40 meters	Sandstone	Aalenian	Shoreface
Not	7.5 meters	Dark grey to black claystone with siltstone lamina	Aalenian	Quiet marine, probably below wave base

Garn	35 meters	Sandstone	Late Aalenian and the Early Bajocian	Near shore with some tidal influence
Melke	212 - 160 meters	Claystones with thin siltstone lamina in between	Late Bajocian to the Early Bathonian	Offshore transitional to lower shoreface

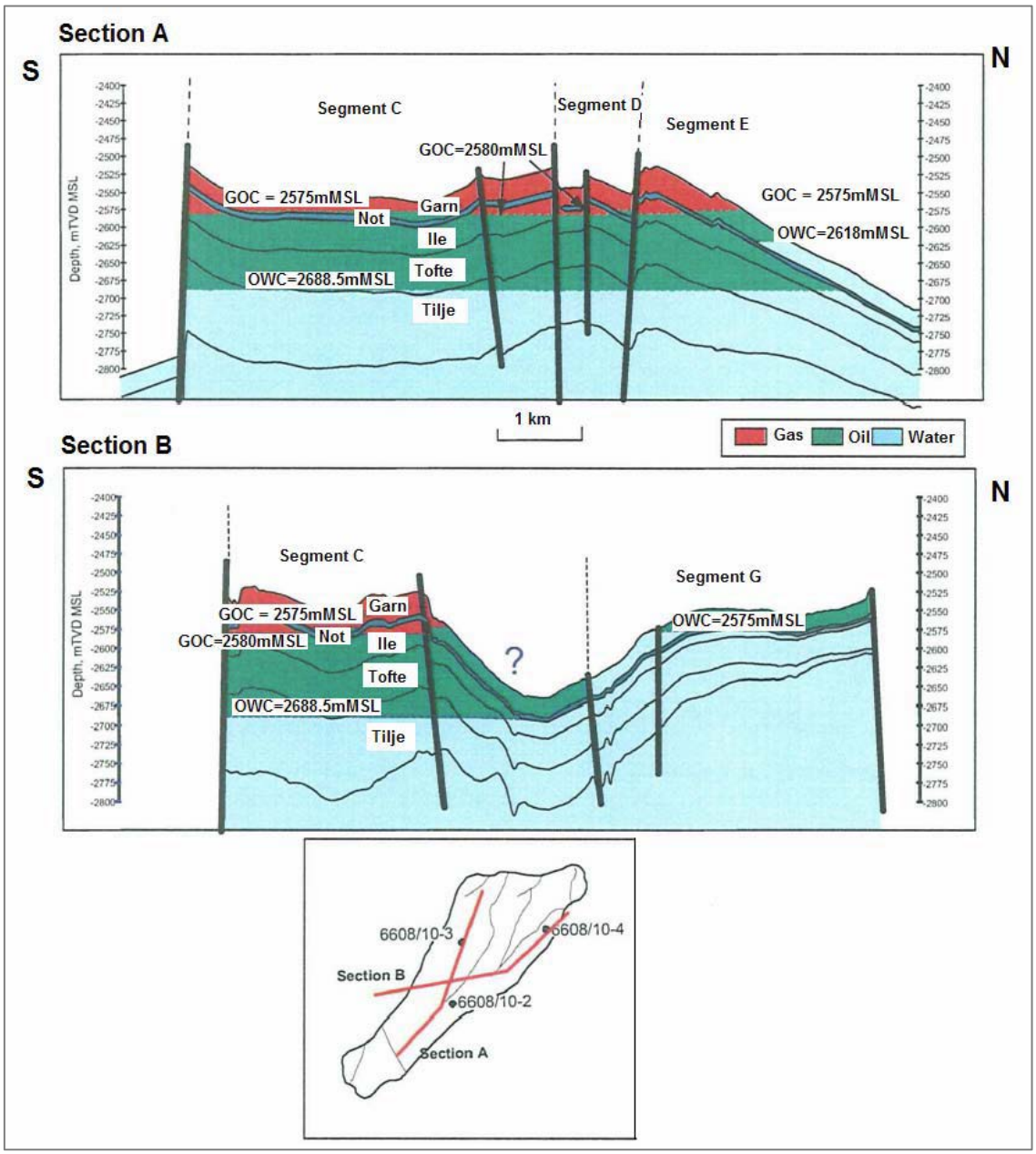

Figure 3.5 – Cross Sections through the Norne Field with Faults and Fluid Contacts [20]

Reservoir communications in this field is affected by both fault and stratigraphic barriers. These two barriers restrict the lateral and vertical fluid flow. Stratigraphic barriers have been identified from logs and cores, while fault can be discovered by interpreting the seismic data. A number of faults presents because the field is located on a horst. The existence of major fault in Norne field including the fluid contacts is illustrated in Figure 3.5.

3.2 Drainage Strategy

As common goal of all oilfields, Norne field was also set to achieve an economic optimum production development. Early stage of the development was maximizing its processing and production. Re-injecting produced gas into gas cap has been implemented until it was discovered that Not formation is actually sealing the Norne main structure from Garn formation. After reaching its plateau production, more wells were drilled, not only vertical wells but also horizontal and deviated wells. Pressure maintenance is applied in the reservoir by injecting water into water zone. Drainage strategy of the Norne field in time scale is illustrated in Figure 3.6. As can be shown in the figure, water is injected into lower Tofte formation up to year 2005, and then produces the oil from Ile and upper Tofte formations.

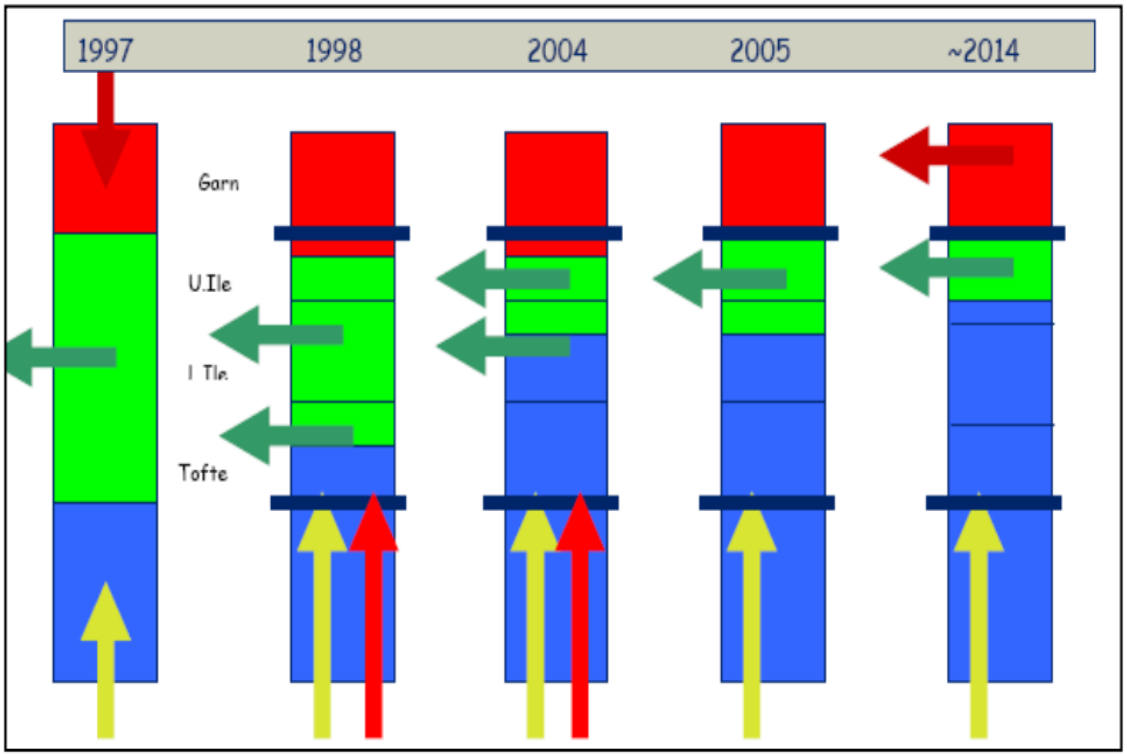

Figure 3.6 – Drainage Strategy of Norne Field [16]

Based on license PL128 [16], reservoir management of the field was concentrated in following points:

- Safe and cost effective drainage of proven reserves
- Prove new reserves at optimal timing to utilize existing infrastructure and exploring the potential in the license
- Adjust capacities in cases where this could be done cost effectively
- Improve drainage strategy with low cost infill wells as multilateral/MLT and through tubing drilled wells/TTRD
- Improved description and optimized drainage strategy to achieve recoverable reserves to more than 90 million Sm^3
- Increase reservoir pressure in Ile Formation at the Norne C-Segment

Currently Norne field is in its tail production or recognized as mature field. Enhanced Oil Recovery (EOR) and Improved Oil Reservoir (IOR) are necessary techniques to obtain higher recovery. Through tubing rotary drilling (TTRD) is performed to create multilateral wells as an addition of conventional infill drilling to drain more oil from the reservoir.

3.3 Full Field Reservoir Simulation Model

Current reservoir simulation model of Norne field is based on 2004 geological model. It uses three-dimensional, three-phase, and full field black-oil model. The model includes all segments of the field consisting 46 x 112 x 22 grids with 49080 active grid cells. Length of each grid in x- and y- directions varies between 80 – 100 meters and the average grid block size is 100m x 95m x 10m. The simulation is set to start in November 6^{th} 1997, and the well data is updated until January 1^{st} 2008.

Full field reservoir model of Norne field is shown in Figure 3.7. Top structure indicates ternary of the first layer (Garn formation in main structure) at initial condition or before production started. The model was constructed by up-scaling the geological and petrophysical models which are porosities, permeabilities, and net-to-gross (NTG).

For reservoir modeling, the entire thickness is divided into 22 zones as listed in Table 3.2. This zonation is not only based on sequence boundaries and maximum flooding surface, but also lithology and porosity/permeability from certain wells. Faults were set by creating specified sections in the model. Transmissibility multipliers were assigned at those sections using keyword MULTZ in z-direction and MULTFLT across a fault using eclipse simulator.

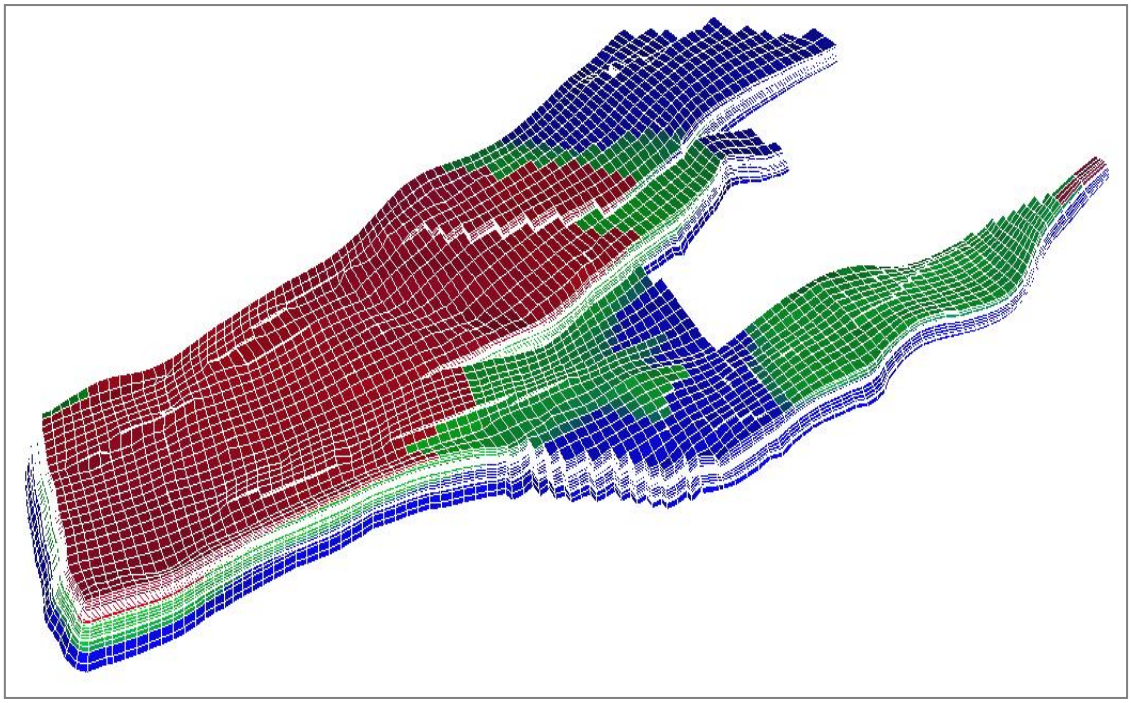

Figure 3.7 – Full Field Reservoir Simulation Model of Norne Field

Table 3.2 – Reservoir Model Zonation of Norne Field [21]

Layer number	Layer name	Layer number	Layer name
1	Garn 3	12	Tofte 2.2
2	Garn 2	13	Tofte 2.1.3
3	Garn 1	14	Tofte 2.1.2
4	Not	15	Tofte 2.1.1
5	Ile 2.2	16	Tofte 1.2.2
6	Ile 2.1.3	17	Tofte 1.2.1
7	Ile 2.1.2	18	Tofte 1.1
8	Ile 2.1.1	19	Tilje 4
9	Ile 1.3	20	Tilje 3
10	Ile 1.2	21	Tilje 2
11	Ile 1.1	22	Tilje 1

CHAPTER 4
EFFECT OF LOCAL GRID REFINEMENT (LGR)

In simulation, refinement is very important technique to get more accurate data. Fewer grids will affect the numerical dispersion that can cause saturation changes rapidly. The more grid number we use, the smaller numerical dispersion will affects the simulation result because the smaller effect of abrupt saturation change can occur. In a grid system, the proportion of fluid flow from one grid to another is a function of average saturation in the upstream grid (as eclipse uses upstream selection). For example in block i+1, probably water has not invaded the block, but since at block i water is above the initial low saturation and have considerable mobility, thus there is more water saturation in block i+1 because the property in block is used to drive the simulation.

In a transition zone, grid definition must be fine enough to characterize the pressure gradient [(22)] .Rapid changes of pressure also occur at the near wellbore area where detail data is needed, hence finer grid block size is required. In generating well testing data from simulation, it is also necessary to have detail pressure data around the wellbore to get more realistic data as real reservoir condition has. So then grid blocks size near wellbore gives considerable impact to pressure response during well testing.

Well D-1H is chosen to conduct the test, located in Norne C-segment (Figure 4.1). It is a vertical well perforated along oil zones in the reservoir, and then conventional well testing analysis can be simply applied. The well is producing from Ile formation (layer 5-7 and 9-11) and upper part of Tofte formation (layer 12-13).

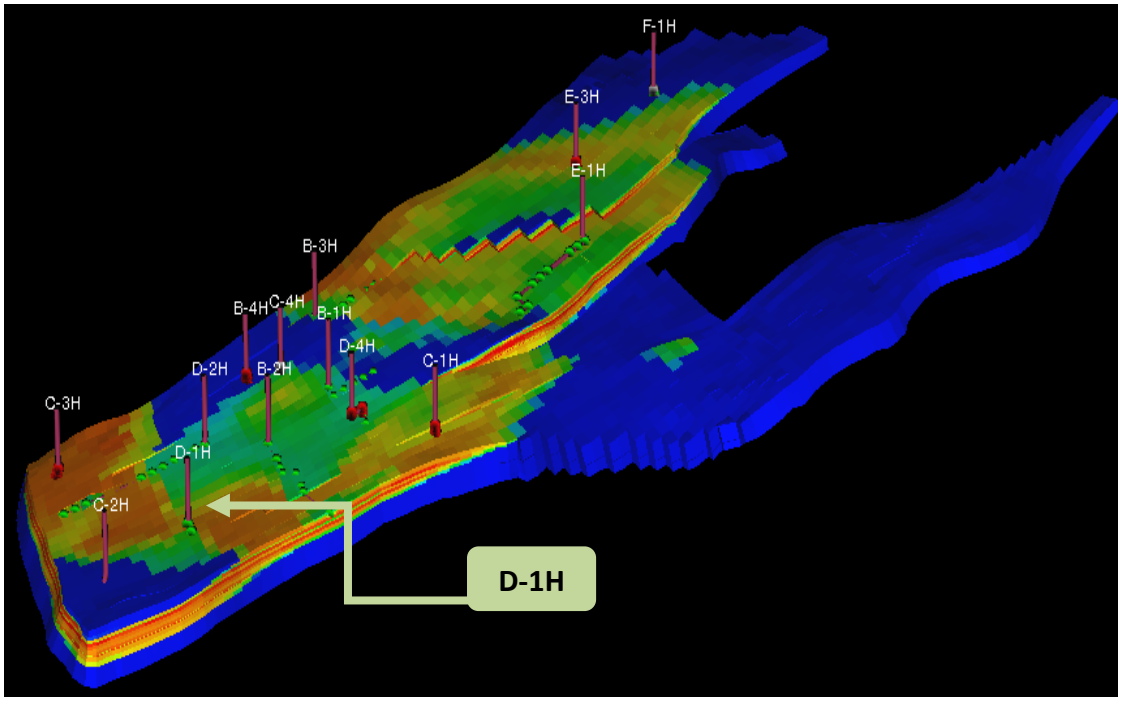

Figure 4.1 – Oil Saturation Map of Norne Field at Layer 6

4.1 Grid Design in Simulation Model

4.1.1 Extension of Local Grid Refinement (LGR) Area

In simulation, several cases can be designed to see the impact of grid block size to pressure response during shut-in period. Base case is set from original reservoir model of Norne field, and the well test data is generated from well D-1H. First case (Case 1) is built by dividing each near wellbore grid into 2 x 2 x 2 finer grid that represents I x J x K direction respectively. The second case (Case 2) is the same dimension as the first case but with larger area covered.

To set those specified gridding system in reservoir model using Eclipse, certain keywords have to be mentioned in .DATA file. It is called Local Grid Refinement (LGR), used to enhance grid definition near wells [23]. In RUNSPEC section, keyword LGR is inserted to specify the maximum number of LGRs in the model and the maximum number of cells in each LGR. Simulator will recognize this keyword as an addition of grids without changing the entire field model dimension which has already specified in DIMENS section. Keyword CARFIN has also to be included in GRID section as the model is Cartesian-based. It specifies column in the global model which is going to be replaced by finer grids. In Norne field reservoir model, those keywords are inserted as following figures (Figure 4.2 and 4.3) for Case 1:

```
LGR
--MAXLGR MAXCLS
  1       4500  /
```

Figure 4.2 – LGR Keyword in RUNSPEC Section

```
--Define a local grid D1H
CARFIN
--Name  I1 I2 J1 J2 K1 K2 NX NY NZ
  D1H   22 24 21 23  5 14  6  6 20  /
ENDFIN
```

Figure 4.3 – CARFIN Keyword in GRID Section

All properties in local grid are set to be the same as the global grid of Norne field reservoir model. Otherwise it should be specified before ENDFIN command. NX, NY, and NZ indicate the number of refined cells along X, Y, and Z directions.

This Local Grid Refinement near wellbore also leads the change of well coordinates and some keywords to place the well in local grids. These changes are applied in SCHEDULE section. WELSPECL will be used instead of WELSPECS; and COMPDAT is changed into COMPDATL (Figure 4.4 and 4.5). Both require additional item – the name of the local grid – before the location coordinates. Below are the modified sections of the first case of LGR (2 x 2 x 2 finer grid blocks size).

```
WELSPECL
-- WELL -- GROUP -- LOCAL GRID -- LOCATION -- BHP -- PREF
-- NAME -- NAME -- NAME -- I J -- DEPTH -- PHASE
'D-1H'   'MANI-D1' 'D1H'   2 3    1*      'OIL'  2*       'STOP'    4*/
/
```

Figure 4.4 – WELSPECL Keyword in SCHEDULE Section

```
COMPDATL
-- WELL -- LOCAL -- LOCATION --- OPEN - SAT - CONN - WELL - KH - S - D - PEN
-- NAME -- GRID -- IX JY K1 K2 -- SHUT - TAB - FACT - DIAM - - - - DRN
  'D-1H'   'D1H'   2  3  2  2   'OPEN'   1*   5.505  0.216    510.312  2* 'Z' 15.511 /
  'D-1H'   'D1H'   3  3  3  3   'OPEN'   1*   0.101  0.216      9.456  2* 'Z' 16.532 /
  'D-1H'   'D1H'   3  3  4  4   'OPEN'   1*   0.101  0.216      9.456  2* 'Z' 16.532 /
  'D-1H'   'D1H'   3  3  5  5   'OPEN'   1*   4.938  0.216    452.905  2* 'Z' 14.704 /
  'D-1H'   'D1H'   3  3  6  6   'OPEN'   1*   4.938  0.216    452.905  2* 'Z' 14.704 /
  'D-1H'   'D1H'   3  3  9  9   'OPEN'   1*   19.086 0.216   1745.284  2* 'Z' 14.493 /
  'D-1H'   'D1H'   3  3  10 10  'OPEN'   1*   19.086 0.216   1745.284  2* 'Z' 14.493 /
  'D-1H'   'D1H'   3  3  11 11  'OPEN'   1*   50.101 0.216   4655.453  2* 'Z' 15.689 /
  'D-1H'   'D1H'   3  3  12 12  'OPEN'   1*   50.101 0.216   4655.453  2* 'Z' 15.689 /
  'D-1H'   'D1H'   3  3  13 13  'OPEN'   1*   8.974  0.216    823.585  2* 'Z' 14.751 /
  'D-1H'   'D1H'   3  3  14 14  'OPEN'   1*   8.974  0.216    823.585  2* 'Z' 14.751 /
  'D-1H'   'D1H'   3  3  15 15  'OPEN'   1*   0.479  0.216     43.304  2* 'Z' 13.707 /
  'D-1H'   'D1H'   3  3  16 16  'OPEN'   1*   0.479  0.216     43.304  2* 'Z' 13.707 /
  'D-1H'   'D1H'   3  3  17 17  'OPEN'   1*   12.603 0.216   1152.420  2* 'Z' 14.489 /
  'D-1H'   'D1H'   3  3  18 18  'OPEN'   1*   12.603 0.216   1152.420  2* 'Z' 14.489 /
/
```

Figure 4.5 – COMPDATL Keyword in SCHEDULE Section

The gridding systems of those 3 cases above are visualized in Figure 4.7, 4.8, and 4.9.

4.1.2 Increase of Local Grid Refinement (LGR) Factor

Additional comparison (Case 3) is made by dividing each near wellbore grid into 3 x 3 x 3 finer grid block size. When the refinement change into this finer grid block size, keyword MINPV in .DATA file should be set with smaller value compare to the value in original model (base case). The keyword is used to declare a threshold pore volume that a cell must exceed [23]. In base case, MINPV is equal to 500. If the refinement is increased, the pore volume in each cell falls below this value, and then it will made inactive. To keep the cells active, in GRID section, the value is reduced as shown in Figure 4.6. With the same area as the first case of 2 x 2 x 2 LGR, 3D view of this model is shown in Figure 4.10.

```
MINPV
  100 /
```

Figure 4.6 – MINPV Keyword in GRID Section

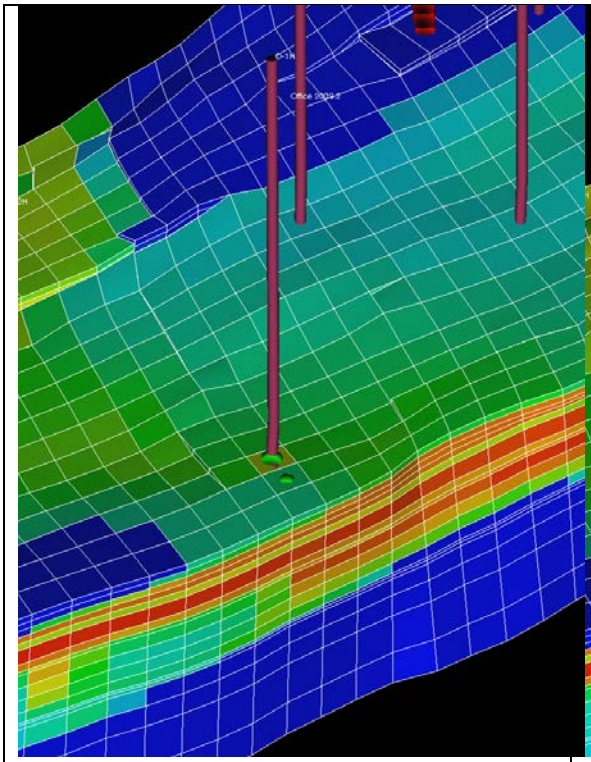

Figure 4.7 – Well D-1H Basecase

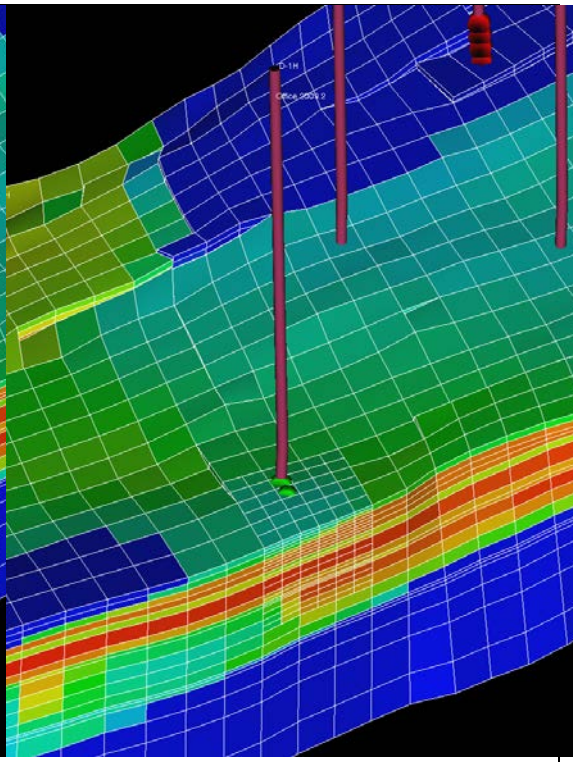

Figure 4.8 – Well D-1H with 2x2x2 LGR Dimension (Case 1)

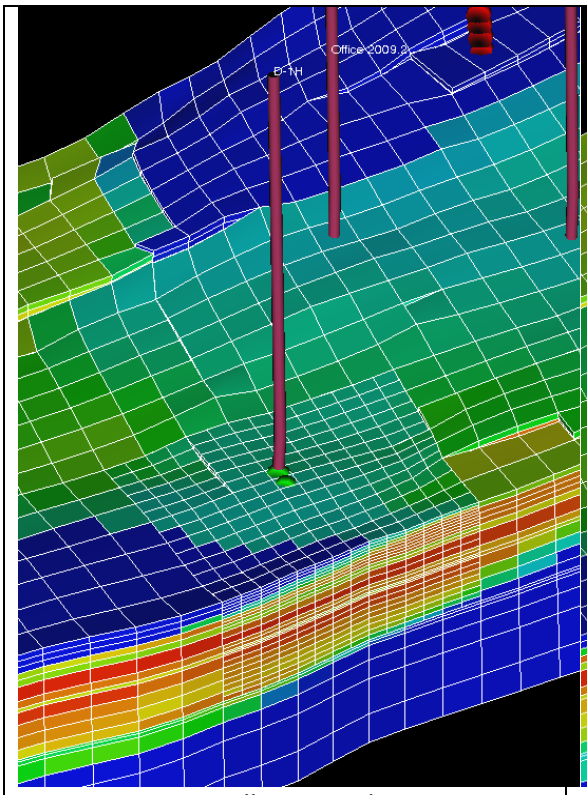

Figure 4.9 – Well D-1H with 2x2x2 LGR Dimension and Larger Area Covered (Case 2)

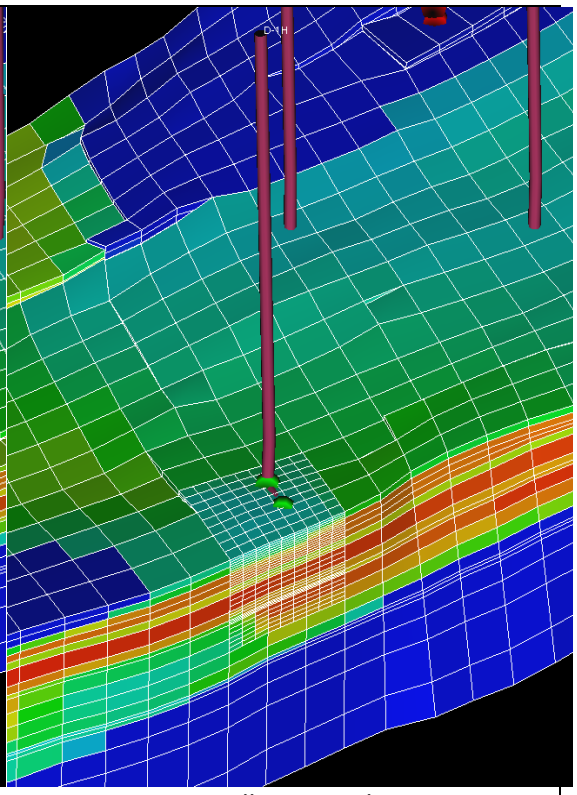

Figure 4.10 – Well D-1H with LGR 3x3x3 Dimension (Case 3)

4.2 Pressure Response from Simulation

For all cases, well D-1H production profiles are modified to generate well testing data. The well is first producing with a constant rate at 24526 BOPD for 10 days (240 hours), and then shut it in more than 300 hours to clearly see the pressure difference. In these sets of data, no injections in Norne field are included during simulation for producers. Figure 4.11 shows generated well test data of D-1H base case. During production, bottom hole pressure is decreasing from 2150 psi to 2115 psi. While the production is zero, pressure significantly increases to 2980 psi and gradually reaches 3210 psi at the end of shut-in period.

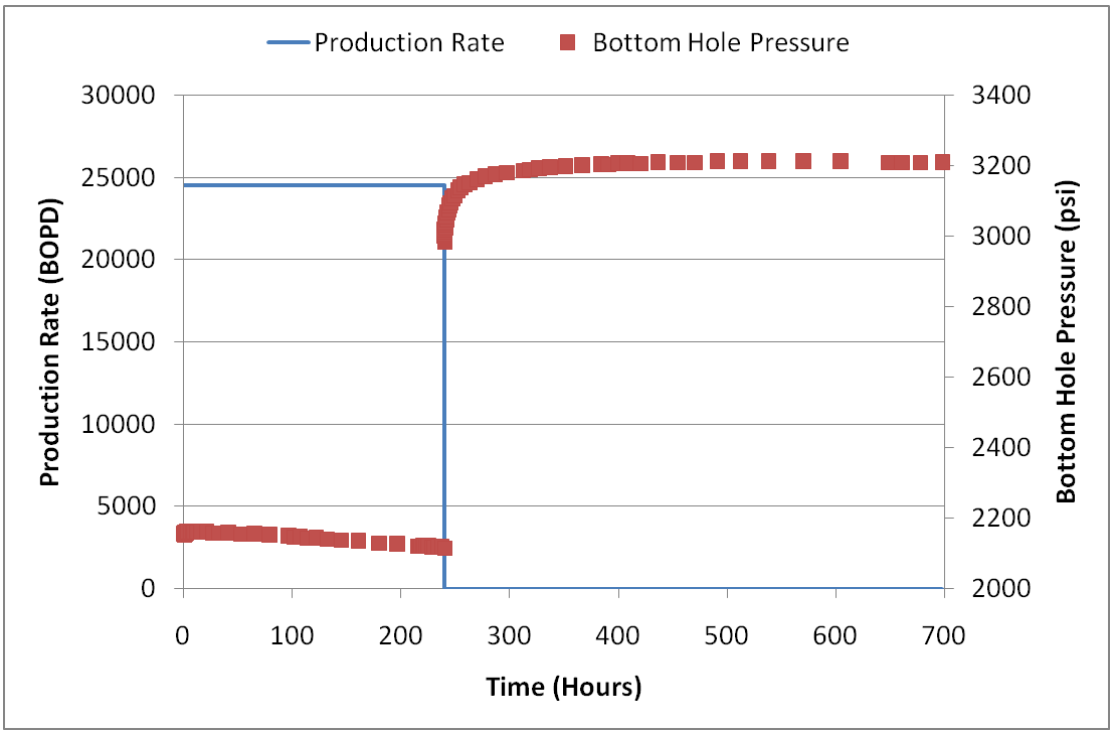

Figure 4.11 – Well Test Data of D-1H (Base Case)

- ***Extension of LGR Area***

The bottom hole pressure (BHP) is recorded during the test. Three different responses are captured in Figure 4.12.

Line D-1H represents base case of Norne field reservoir model, while D-1H_RFN indicates the first case of 2 x 2 x 2 LGR (Case 1). The case of larger LGR area (Case 2) is presented by D-1H_RFN1 line. Figure 4.12 shows that LGR gives higher pressure response compare to the base case; and extended area of LGR results much higher bottom hole pressure. Case 1 and 2 have a significant difference after 20 hours up to 150 hours, then getting converged after 250 hours of shut-in period. It indicates that wider area of LGR gives significant changes of bottom hole pressure of a well. Wider LGR area is also related to radius of investigation of a well testing; and this radius can be correlated to shut-in time (Equation 2.4). Outside this radius of investigation, LGR might not give any impact.

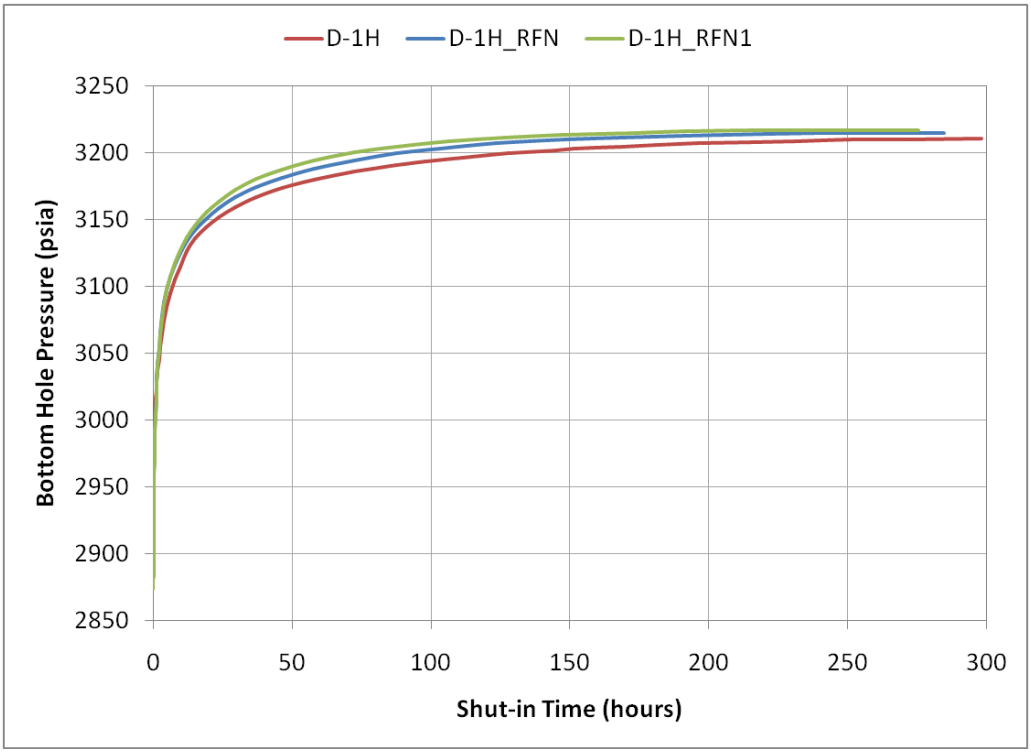

Figure 4.12 – Shut-in Pressure of Well D-1H (Base case, Case 1, and Case 2)

For 150 hours of shut-in time, the radius of investigation is calculating as below:

$$r_{inv} = \sqrt{\frac{kt}{948\emptyset\mu c_t}} = \sqrt{\frac{(181)(150)}{948(0.26)(0.5)(1.4x10^{-5})}} = 3950\ ft$$

This case might give information that LGR should be applied for radius 3950 ft from the observation well.

- ***Increase of LGR Factor***

Figure 4.13 shows effect of local grid refinement increase. The area covered for these LGR cases are the same. D-1H_RFN line is presenting 8 equally divided smaller cells from each grid blocks, and D-1H_RFN3 represents 27 finer cells from each near wellbore grid blocks. Slightly visible difference observed at the time less than 40 hours. It implies that finer grid is really sensitive at early time of well testing near wellbore. So, when generating well testing data from simulation, one of issue to be considered is to have finer grid near the wellbore. Local grid refinement increment might be stopped when no pressure difference produced. Since the shut-in time can be converted to radius of investigation, so then LGR area is easily to be determined.

Radius of investigation for 40 hours testing period is 2040 ft, as calculated bellow:

$$r_{inv} = \sqrt{\frac{kt}{948\emptyset\mu c_t}} = \sqrt{\frac{(181)(40)}{948(0.26)(0.5)(1.4x10^{-5})}} = 2040\ ft$$

It implies that much finer grid (in this case is 3 x 3 x 3 LGR dimension) gives more accurate pressure response for the radius 2040 ft. More than this distance, 2 x 2 x 2 LGR dimension results the same value with shorter time in simulation because less equations will be calculated.

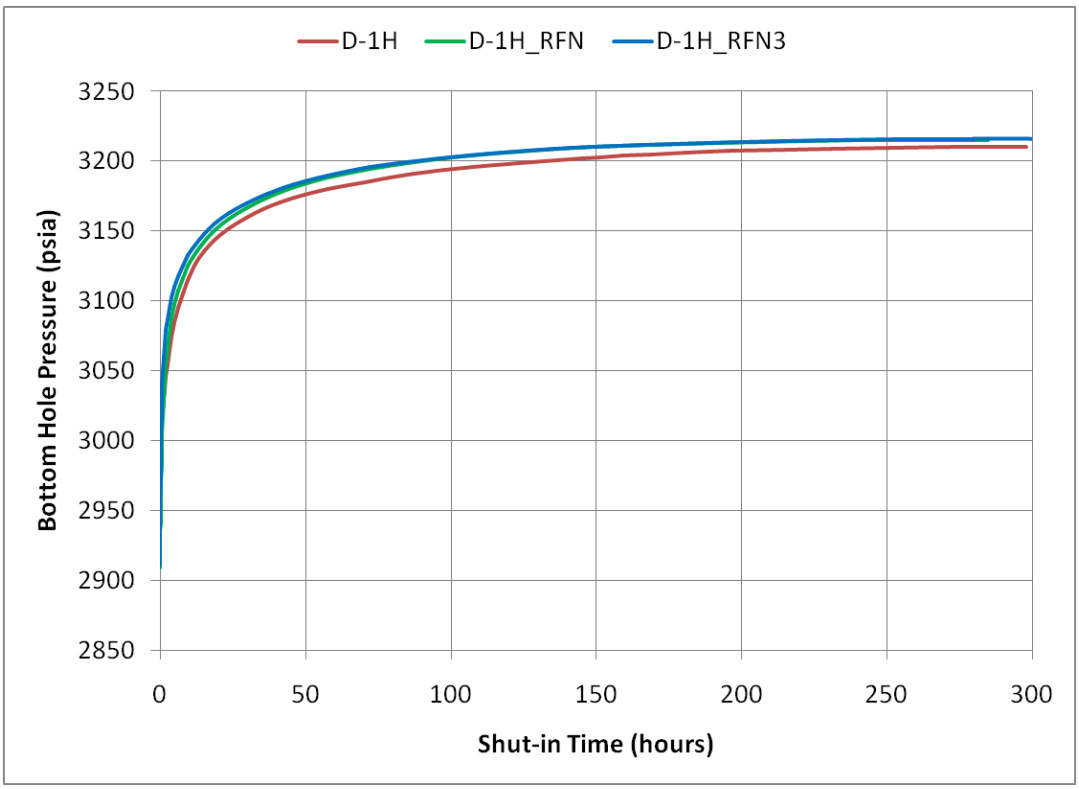

Figure 4.13 – Shut-in Pressure of Well D-1H (Base case, Case 1, and Case 3)

4.3 Analysis Using F.A.S.T Welltest™ Software

As pressures between cases described above have different responses, consequently pressure transient analysis for each case will also have different interpretations. To distinguish the significance impact of pressure deviation to the well testing results, pressure transient analysis using software from Fekete is conducted. Since pressure recorded during shut-in period which represents buildup test, hence permeability and storage capacity are possible to calculate from the buildup analysis. Only oil phase is considered in the analysis as simplification purpose in comparing various cases. Radial flow analysis is applied where this type of flow exists before the pressure transient has reached the reservoir boundary, called as infinite-acting reservoir.

Results of each case are tabulated in Table 4.1. Calculations in software are based on theoretical equation mentioned in Chapter 2 (Equation 2.11 and 2.10). All the horner plot and derivative plots are available in Appendix A.

Table 4.1 – Analysis Results of All Cases

Case	Plot Line Legend	Permeability (mD)	Storage Capacity (bbl/psi)	Extension of LGR Area Comparison	Increase of LGR Factor Comparison
Basecase	D-1H	181	16.9	Yes	Yes
Case 1	D-1H_RFN	169	4.2	Yes	Yes
Case 2	D1H_RFN1	158	4.1	Yes	
Case 3	D1H_RFN3	171	2.5		Yes

Supporting data for this analysis is tabulated in Table 4.2:

Table 4.2 – Additional Reservoir and Well Data of D-1H

Parameter	Value	Unit
q_o	24500	BOPD
μ_o	0.5	cp
B_o	1.32	RB/STB
h	184	ft
P_{wf}	2058	Psi
Φ	0.2636	fraction
c_t	1.40×10^{-5}	1/psi
r_w	0.3	ft
P_i	3959.5	Psi

- ***Extension of LGR Area***

From Table 4.1, Case 1 has the permeability 7.1 % lower than base case, but 6.5 % higher than Case 2. Associated with pressure graph in Figure 4.12, Case 1 and Case 2 lines are separated after 20 hours of shut-in time that is when permeability analysis is mainly concerned; while base case is separated much earlier. This further suggests that LGR area extension is important to obtain more accurate permeability calculation. On the other hand, since there is no significant pressure difference before 20 hours between Case 1 and Case 2, so then their storage capacities are relatively the same (4.2 and 4.1 bbl/psi). It is because of the same refinement dimension of both cases (2 x 2 x 2). Huge storage capacity from base case (16.9 bbl/psi) is surely due to bigger grid block size near the wellbore. Those storage capacity results are in accordance with theory of wellbore storage calculation which is analyzed at early time of shut-in period.

- ***Increase of LGR Factor***

Correlates to Figure 4.13, starting from 40 hours of the tests, both Case 1 and Case 3 are getting converges that means permeability calculation might be similar. It is confirmed from software analysis that results almost the same permeability for both cases which are 169 mD and 171 mD, respectively. Even though they tend to be in the same line, but still there is visible pressure difference before 40 hours that obviously reflects on the wellbore capacity prediction. Case 3 has much smaller storage capacity (2.5 bbl/psi) as the impact of having finer cells along the well and its surrounding; furthermore it is better to reflect actual reservoir condition. It is even more convincing that the smaller grid is important to do for wellbore storage or early time analysis when generating well testing data from simulation.

CHAPTER 5
INTERFERENCE TEST ACROSS THE FAULT

This chapter discuss about interference test that involves three wells during the test. The selected observation well is E-3H, a vertical well located in E-Segment. There are two offset producers; E-1H and E-2H, both are horizontal wells. Well E-2H is drilled in E-Segment, while E-1H is in D-Segment. A major fault lies between those two offset wells, as a border of the two segments. Location of the wells in Norne field can be seen in Figure 5.1.

Since the interfering wells located in different segment separated by a fault, interference test might become one of the analyses to evaluate communication between D- and E-Segments. It will be influenced by pressure response in observation well and also production rate of the nearest producers. Type curve matching of interference test is possible to perform to calculate permeability. Before performing interference test analysis, conventional buildup analysis will also be conducted to determine permeability using Fekete software. Then, this permeability value will be used to calculate pressure drop in observation well affected by producing wells. For simplification purpose, all analyses are performed by only consider the oil production. In actual field case, multiphase flow might commonly exist which lead a very complex analysis.

All the three wells were perforated in Ile formation. Most of the formation was vertically penetrated by well E-3H. Middle formation of Ile in E-Segment is drained from well E-2H, at the same time well E-1H is producing from top to middle of Ile formation in D-Segment. Thus, it is assured that interference test between those specified wells above is one of valuable method to investigate.

5.1 Well Test Data from Simulation

As discussed in previous chapter, near wellbore is the area where rapid change of pressure might occur. Then, the same technique of Local Grid Refinement (LGR) is implemented at E-3H. This LGR area is shown in Figure 5.1. Along the perforation intervals are refined in radius 2 grid blocks from the well. After having several simulations about LGR for this well, finally 2 x 2 x 2 dimension of LGR is applied during the test which can represent a good analysis.

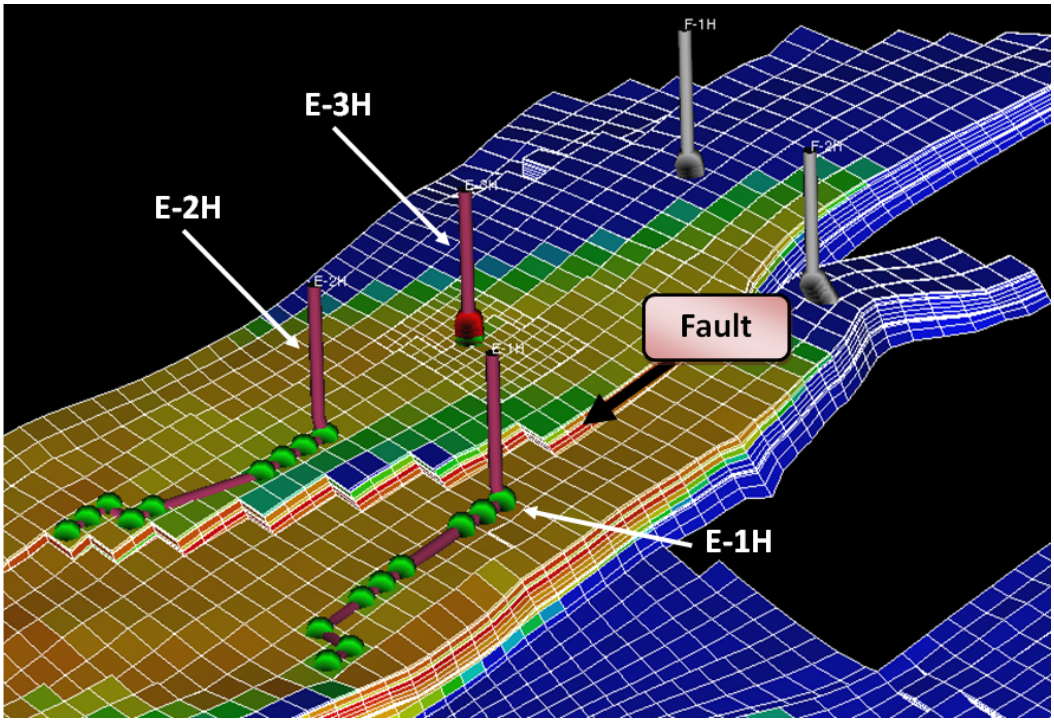

Figure 5.1 – Well E-3H with LGR in E-Segment

To provide buildup data, well E-3H is first being produced with constant rate for ten days, and then shut it in for 24 hours. The pressure response during shut-in period is only considered in buildup analysis. Shut-in is continued to longer time up to 500 hours to generate interference test data. E-3H will receive some interference from surrounding producers (E-1H and E-2H) during this extended time of shut-in. In these sets of data, no injections in Norne field are included during simulation for producers. Reservoir model of Norne field used in this study has been matched with production history, so in assumption that the analysis is referred to actual reservoir condition.

Well test data of E-3H is plotted in Figure 5.2. Oil production rate is maintained at 11800 BOPD with bottom hole pressure decreasing from 1887 psi to 1763 psi. While the production is zero, pressure significantly increases to 2704 psi and gradually reaches 3022 psi, then as affected by offset wells productions, the pressure is back to decrease.

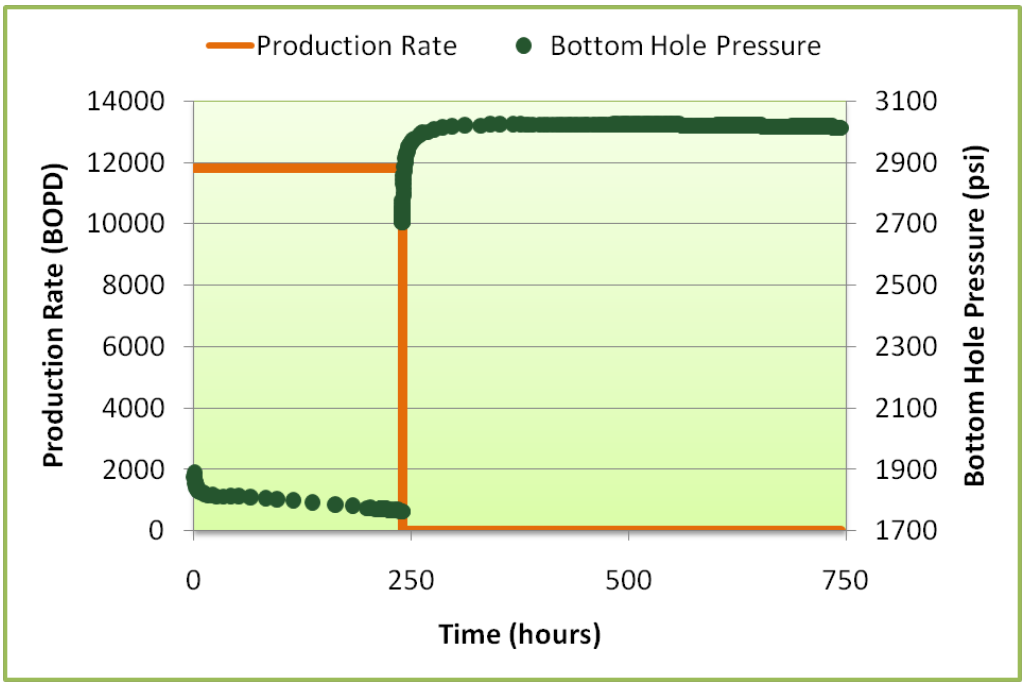

Figure 5.2 – Well Test Data of E-3H

5.2 Permeability Determination

Several methods to determine permeability are applicable in pressure transient analysis. Comparing the results of different methods is also necessary to investigate. Better estimation of permeability will be obtained using well test data of shut-in period since it has stable response compare to drawdown test that produces high turbulence. In this sub-chapter, buildup and interference analysis of well E-3H are performed, and then interpret permeability results from both techniques. Permeability estimated from these analyses will be operated for the calculation of pressure drop in sub-Chapter 5.3.

5.2.1 Buildup Analysis

Radial flow analysis is applied in this method, it means that the flow exists before the pressure transient has reached the boundary of the reservoir, it is also called infinite-acting reservoir. The test requires only one well as observation well (individual well testing). On semi-log plot of pressure versus time, straight line will be formed from the data.

This buildup analysis is performed using FAST Welltest^{TM} software from Fekete Company. Figure 5.3 is horner plot that used in interpretation of several reservoir parameters. Straight line started after 10 hours of shut-in indicates that reservoir start to reach the average pressure, and it is where the radial interpretation being analyzed.

Average pressure *p** obtained at 3079 psi and straight line slope *m* is 81.77 psi/cycle. Additional reservoir and well data of E-3H involved in calculation is provided in Table 5.1. Permeability estimation technique of this software is based on Equation 2.11 that explained in Chapter 2. Finally, it results 205 mD of effective permeability.

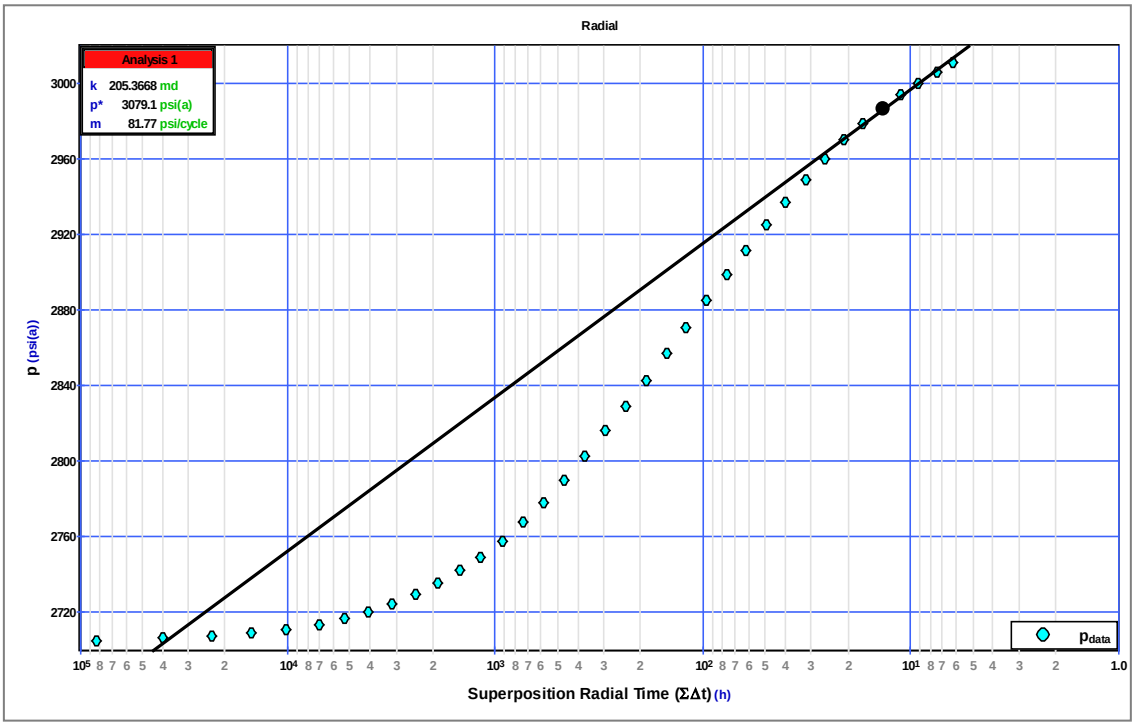

Figure 5.3 – Horner Plot of Well E-3H

Table 5.1 – Additional Reservoir and Well Data of E-3H

Parameter	Value	Unit
q_o	11800	BOPD
μ_o	0.5	cp
B_o	1.32	RB/STB
h	75.5	ft
P_{wf}	1788	Psi
Φ	0.2636	fraction
c_t	$4.7x10^{-5}$	1/psi
r_w	0.35	ft
p_i	3959.5	Psi

5.2.2 Interference Analysis – Type Curve Matching

To estimate effective permeability of the reservoir, type curve matching is one of practical approach in interference analysis. Infinite-acting reservoir behavior is still applied in this method. For this type of test, more than one well is needed (multiple well testing). E-3H acts as observation well which is shut-in during the test, while other

producers keep producing. Figure 5.4 shows pressure data for interference test in well E-3H. It took more than 20 days of shut-in to generate the data to receive significant influence from surrounding flowing producers.

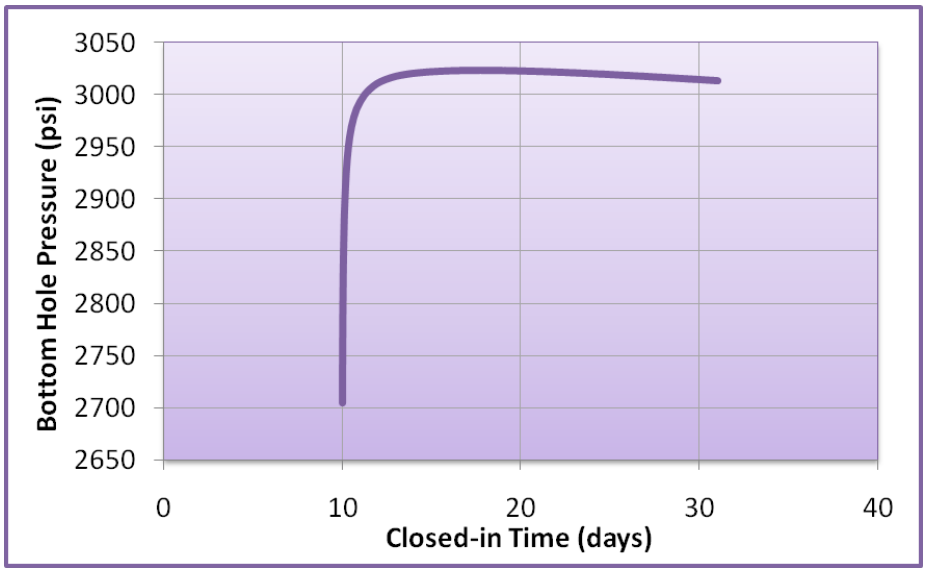

Figure 5.4 – Pressure Data of E-3H Interference Test

Pressure drawdown $Pi\text{-}P_{wf(t)}$ versus time t of observation well is plotted, continued by fitting it to Exponential Integral Solution Type Curve (Figure 2.11) in Chapter 2. Having match point from the plot, then permeability can be calculated using Equation 2.18. Type curve matching of E-3H interference test including the match point is shown in Figure 5.5.

The matched points are:

$(P_D)_{MP}$ = 1
$(\Delta P)_{MP}$ = 145 psi

Then permeability is calculated as follow:

$$k = 141.2\frac{23526(0.5)(1.32)}{75.5}\frac{1}{145} = 200\ mD$$

The above calculation is first assumed that only well production q of E-2H is contributed in the equation due to the existence of fault between the two interfering wells. The assumption then followed by similar result of permeability from buildup analysis result. It convinces that E-2H is the most interfering well to the observation well (E-3H) since they are in the same segment and have similar reservoir property in Ile formation. There is still 2.4 % permeability deviation between interference and buildup analysis result. It might indicate that the fault is not fully-sealed because of the occurrence of some communication between the segments.

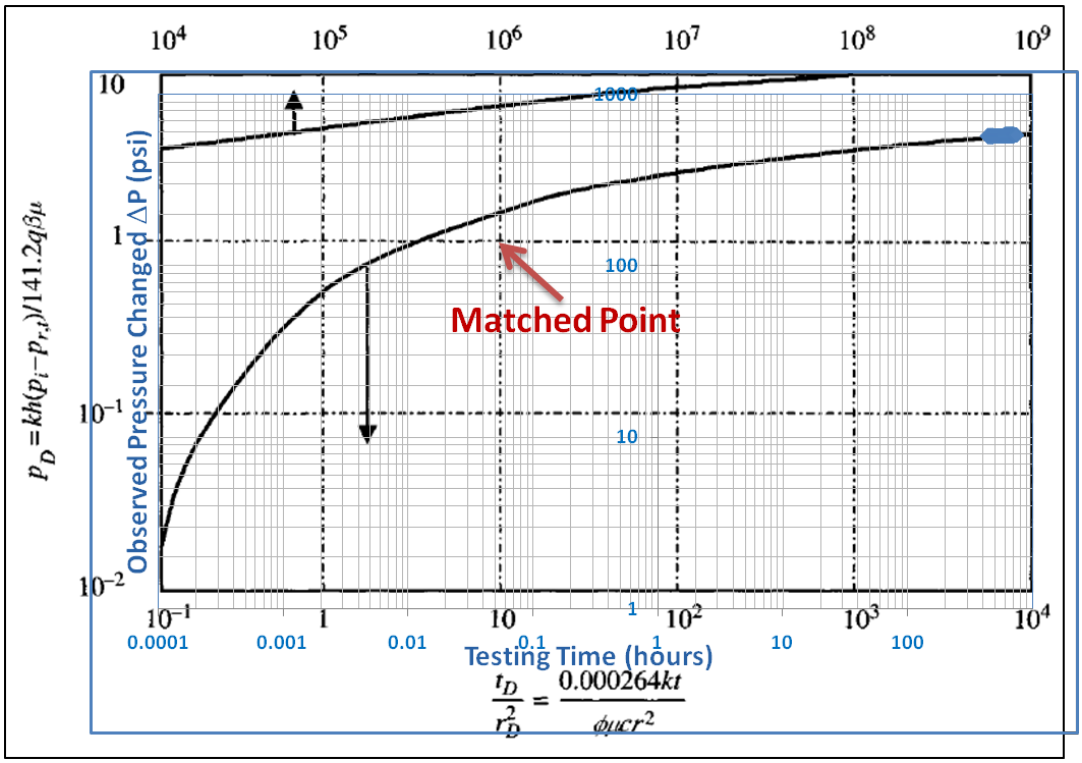

Figure 5.5 – Type Curve Matching of E-3H Interference Test

5.3 Pressure Drop in Observation Well

Pressure drop experienced by the observation well can also determine whether two or more wells around it have a communication with observation well itself. Existence of the fault that separates E-1H from E-Segment may give zero or small pressure drop at well E-3H. This pressure drop is calculated using Equation 2.14. Oil rate of producing wells and their distance to E-3H is tabulated in Table 5.2. Slope *m* is equal to 66 psi/cycle obtained from plot of bottom hole pressure versus (t+Δt)/Δt at observation well as can be seen in Figure 5.6. Production rate of observation well prior to shut-in, *q*, is equal to 11800 BOPD and additional data used in this calculation is provided in Table 5.1. Permeability used is 203 mD as an average of the results from buildup and interference analysis.

Table 5.2 – Oil Rate of Offset Wells and Distance from Well E-3H

Well	Oil Rate (BOPD)	Distance (ft)
E-1H	23300	3050
E-2H	24400	2362

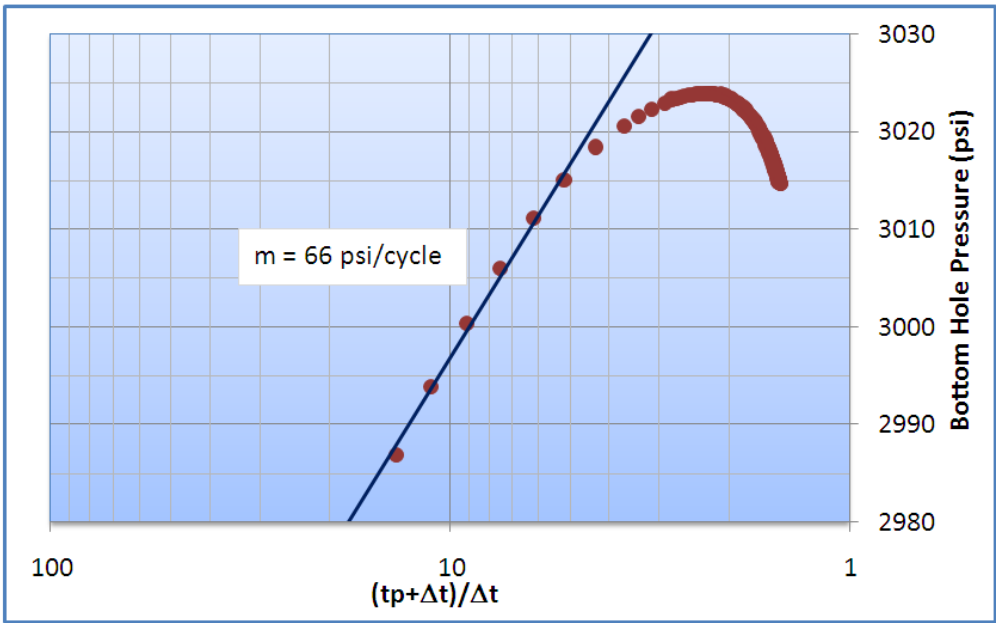

Figure 5.6 – Log Time Plot of E-3H Interference Test

Calculated pressure drop at the observation well caused by production of well E-2H at $\Delta t_j = 0$ is:

$$\Delta p = \frac{-m}{2.303}\left[\sum_{i=1}^{NW}\frac{q_j}{q}\left\{Ei\left(\frac{-\Phi\mu c a_j^2}{0.00105k\left(t_j+\Delta t_j\right)}\right)-Ei\left(\frac{-\Phi\mu c a_j^2}{0.00105k\,t_j}\right)\right\}\right]$$

$\Phi\mu c/k = 3.07\text{x}10^{-8}$

$$\Delta p = \frac{-66}{2.303}\left[\frac{24400}{11800}\left\{Ei\left(\frac{-3.07\times10^{-8}\times2362^2}{0.00105(375+0)}\right)\right\}\right] = 37.6\,psi$$

Complete result of pressure drop during the interference test is shown in Figure 5.7. Based on Figure 5.7, E-2H gives higher pressure drop because it is located in the same segment as observation well (E-3H) and also has relatively closer distance. Production rate of E-2H is slightly higher than E-1H. Although E-1H is located across the fault and further than E-2H, but it still affects the pressure drop in E-3H. Again, it indicates that there is a communication between D-Segment and E-Segment, and the fault which separates them is not fully-sealed.

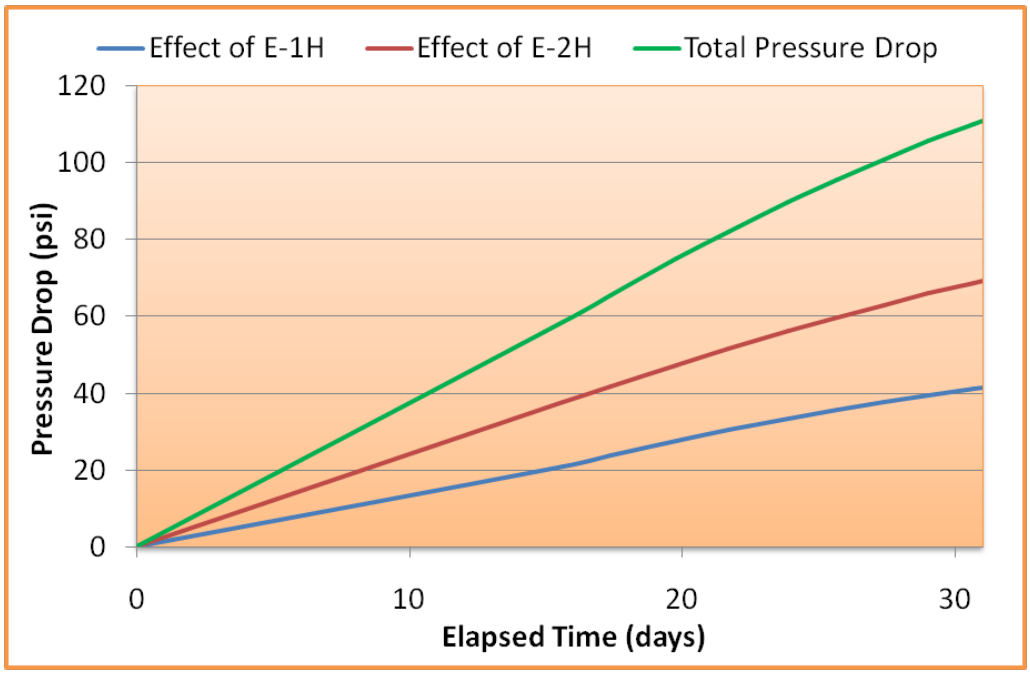

Figure 5.7 – Well E-3H Pressure Drop Affected by Offset Producers

Above investigation is supported by Figure 5.8 that shows pressure trend of those three wells during production period or before the test was started. Different trend of well E-1H from the other two wells clarifies that E-1H is on a different segment or different rock and fluid properties.

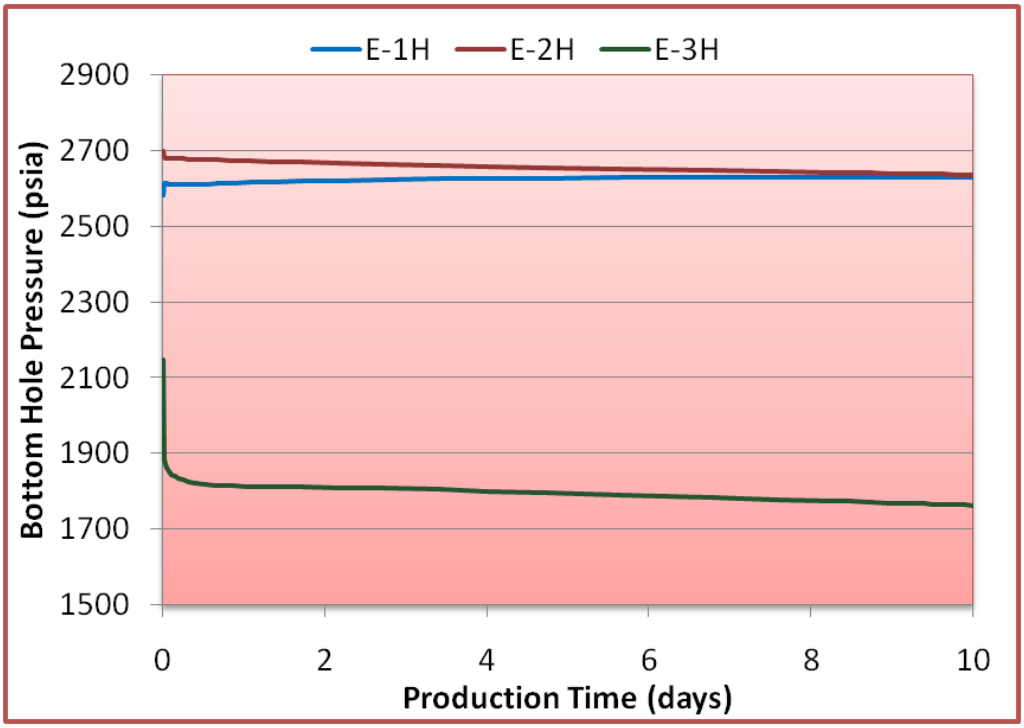

Figure 5.8 – Pressure of Active and Observation Wells during Production

Moreover, production trend of offsets producers during shut-in gives additional interpretation, as shown in Figure 5.9. By shutting-in well E-3H, production of well E-2H is clearly increasing without any injections where fluid in E-Segment concentrated to flow through E-2H. In contrary, well E-1H has decreasing production trend as the continuation of well production decline profile. It is an evidence that well E-1H receives no or small impact of E-3H shut-in because less fluid flows across the fault.

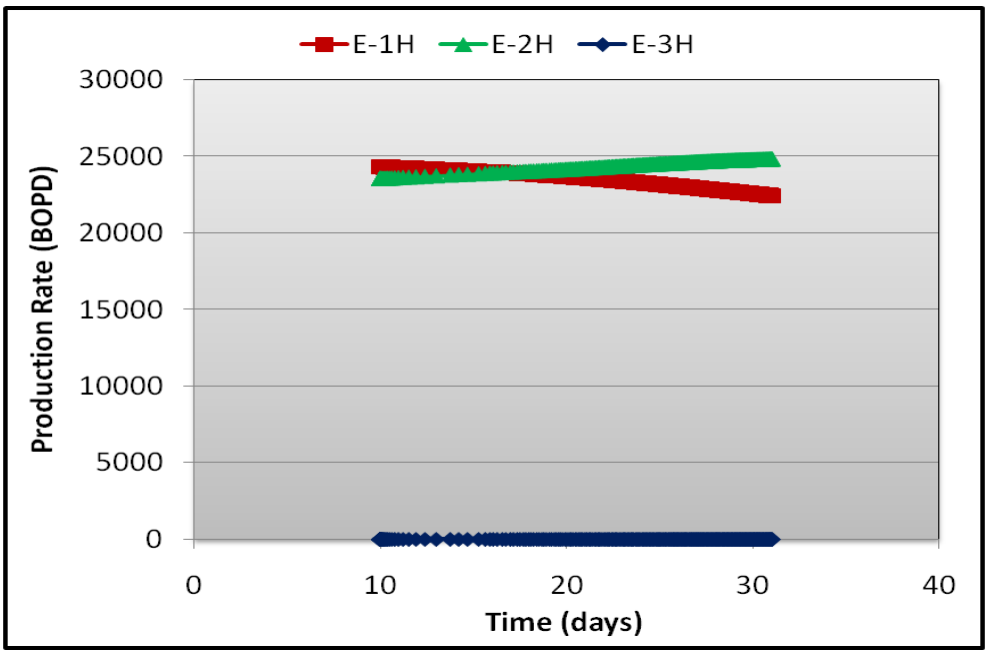

Figure 5.9 – Production Rate of Offset Producers during Shut-in

CHAPTER 6
TRANSIENT WELL TESTING IN HORIZONTAL WELL

Many horizontal wells were drilled in Norne field as a strategy to get significant oil production enhancement. This technique allows wider surface area of oil to be drained towards the wellbore. In this chapter, transient well testing of horizontal well in G-segment of Norne field will be discussed. This segment has relatively thin layer of reservoir compare to other segments, but it has considerable wide area, hence horizontal well is an advantageous approach to produce more hydrocarbon from this part of field.

Well E-4AH is the selected well that acts as main producer in G-segment. This well is placed at 5-10 meter TVD below the top of Garn formation. Figure 6.1 shows the ternary map of Norne field at layer 2 including the location of well E-4AH (in white circle line). Different from the other part of the field, Garn formation in G-segment is mainly saturated by oil with limited amount of gas at the edge of the reservoir as can be seen in the map.

Discussion in this chapter will begin with data generated from simulation, and then analyze those data using manual calculation and software utilization. Transient well testing in horizontal well has specific characterization. Particular stages of flow regimes will be observed and it reflects distinct fluid movements towards the wellbore. Combination of pressure response and derivative analysis will also conducted to facilitate more clearly interpretation.

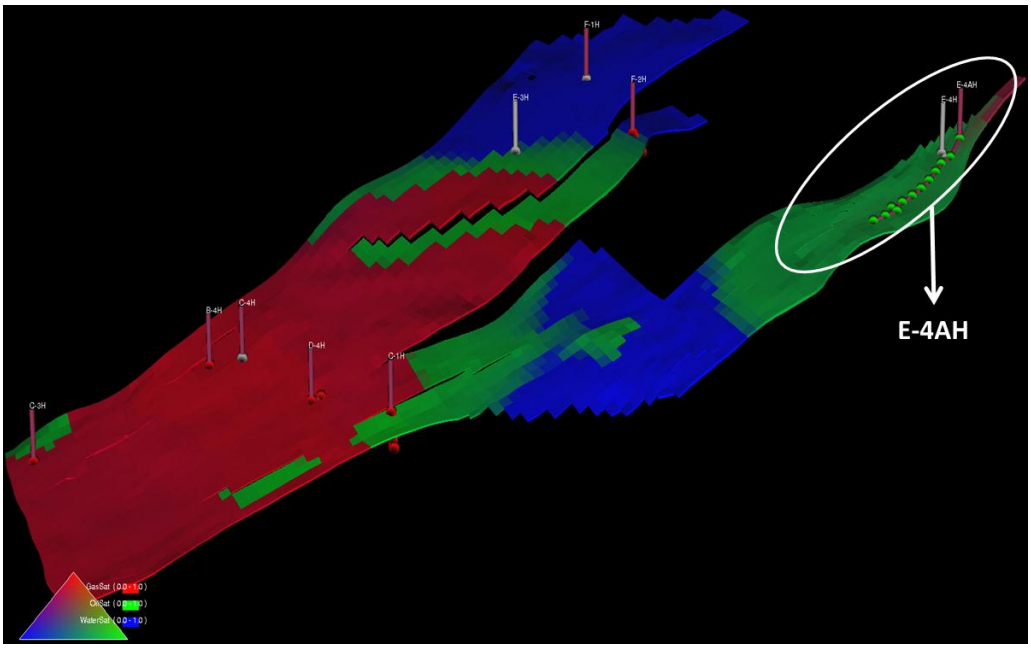

Figure 6.1 – Ternary Map of Norne Field at 2ndLayer and Well Location of E-4AH

6.1 Generated Well Test Data of Horizontal Well in G-Segment

Before generating well test data from simulation, local grid refinement around well E-4AH was applied in the reservoir model. Each block size is divided into 8 finer grids with 2 x 2 x 2 dimension in x, y, and z directions. Well E-4AH with LGR in G-segment is shown in Figure 6.2.

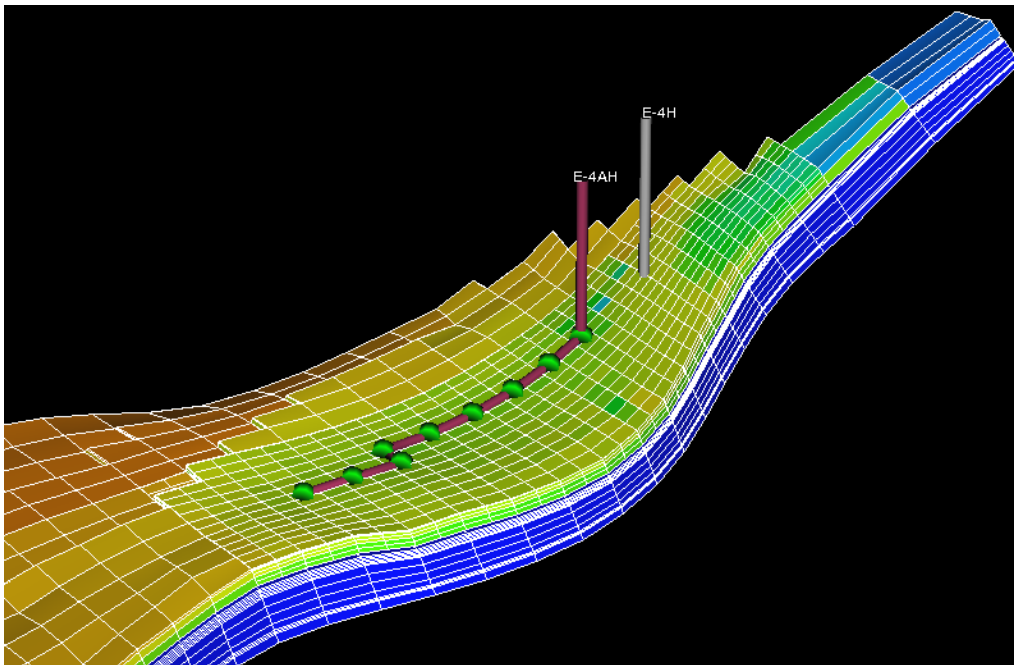

Figure 6.2 – Well E-4AH with LGR in G-Segment

Regarding the test schedule, similar with other cases in previous chapters, well E-4AH is first being produced for 10 days at a constant rate around 32.4 x 10^3 BOPD. The test is followed by shutting-in the well for approximately 24 hours. Production profile and pressure response during the test is plotted in Figure 6.3. Also note that no injectors are activated during the test. Bottom hole pressure response during shut-in period will then process to flow regime analysis. The analysis assumes a single phase system (which is oil) as a simplification of this study. To have a proper comparison with vertical well in Chapter 4 and 5, so buildup test will also conduct at this horizontal well.

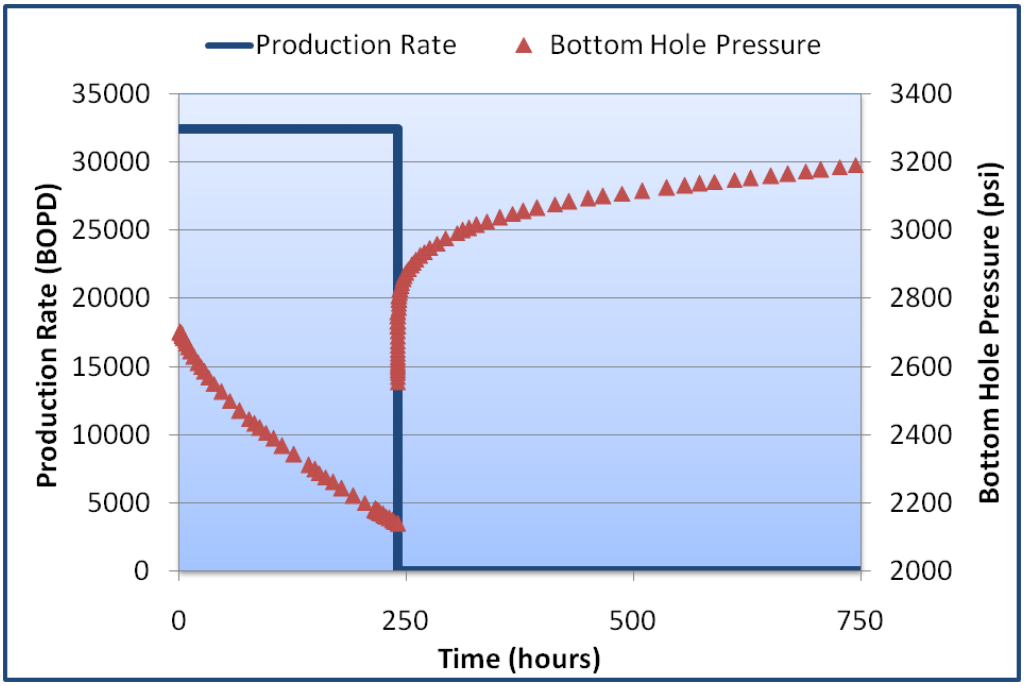

Figure 6.3 – Well Test Data of E-4AH

During constant rate of production, pressure is significantly decreasing from 2700 psi to 2140 psi. It is a huge pressure drop compare to well testing at well D-1H and E-3H (vertical wells). After shutting-in the well, bottom hole pressure immediately jump to 2570 psi then increasingly reach 3200 psi at the end of the test.

6.2 Buildup Analysis in Horizontal Well

First analysis of buildup test in horizontal well is conducted by pressure versus time plots. Analyzing this pressure response of buildup test, two flow regimes are observed; Early-time Radial Flow (ERF) and Intermediate Linear Flow (ILF). Each flow regimes is treated in different plots and formulas as explained earlier in Chapter 2.4. Late-time Radial Flow (ERF) does not appear in this test, so pressure at infinite shut-in time cannot be correctly predicted.

6.2.1 Early-Time Radial Flow Analysis

Conventional horner plot is carried out in vertical radial flow regime. Semilog plot of horner time *(tp+Δt)/Δt* versus bottom hole pressure results a straight-line with slope m_{1r} is 100 psi/cycle. The horner plot is provided in Figure 6.4 including the trend line of ERF (red line). During this regime, fluid flows in vertical direction, and ends when upper and lower boundaries are reached. Based on below figure, vertical radial flow is ended at horner time equal to 20, or after 12 hours of shut-in.

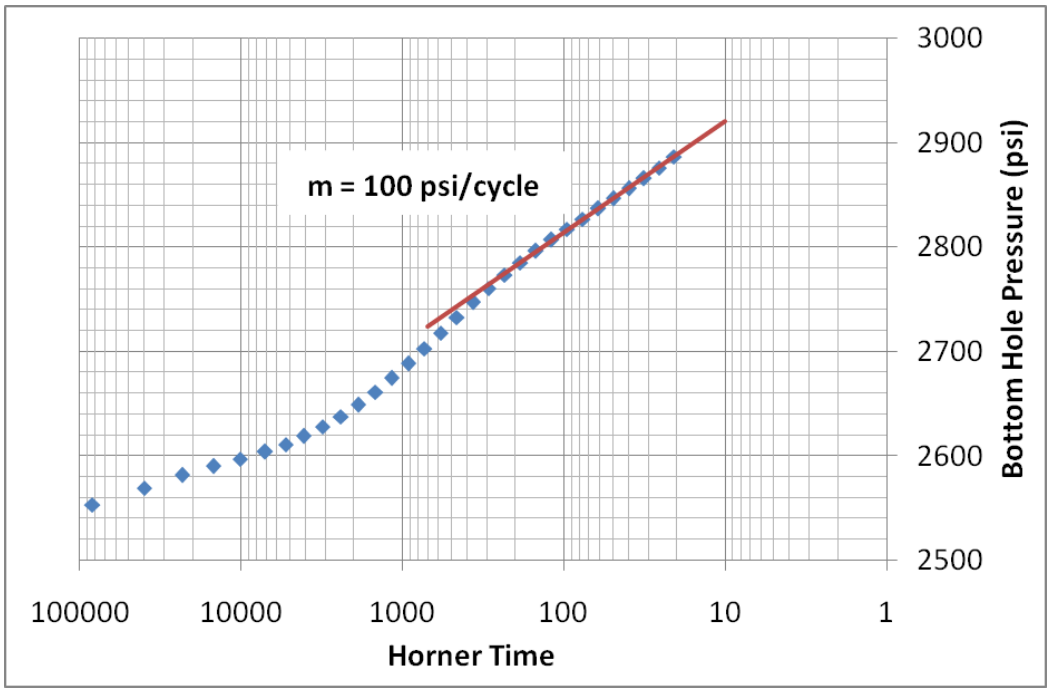

Figure 6.4 – Horner Plot of Early Time Radial Flow

The main purpose of analyzing this flow regime is to estimate vertical permeability since the fluid in the reservoir flows in vertical plane. Refer to Equation 2.32, vertical permeability k_{vy} can be calculated as

$$k_{vy} = 162.6\frac{q\mu B}{m_{1r}L} = \frac{162.6(32393)(0.5)(1.32)}{(100)(4252)} = 8.2\ mD$$

Data required for above calculations are available in Table 6.1.

Table 6.1 – Additional Data for ERF Analysis

Parameters	Value	Unit
B_o	1.32	RB/STB
L	4252	ft
q_o	32393	BOPD
μ_o	0.5	cp

Further discussion about permeability obtained from this analysis and in addition to other results will be presented in next sub-chapter.

6.2.2 Intermediate-Time Linear Flow Analysis

Linear horizontal flow is a transition flow regime between vertical radial flow and horizontal radial flow regimes. It indicates that flow from top or bottom of reservoir has reached the wellbore. To investigate the presents of this flow regime, a plot of bottom hole pressure versus square root of time should be generated. Figure 6.5 shows the plot and deliver a straight-line with slope m_{1l} is 30 psi/cycle. The plot also shows that intermediate-time linear flow is ended after 36 hours of shut-in period.

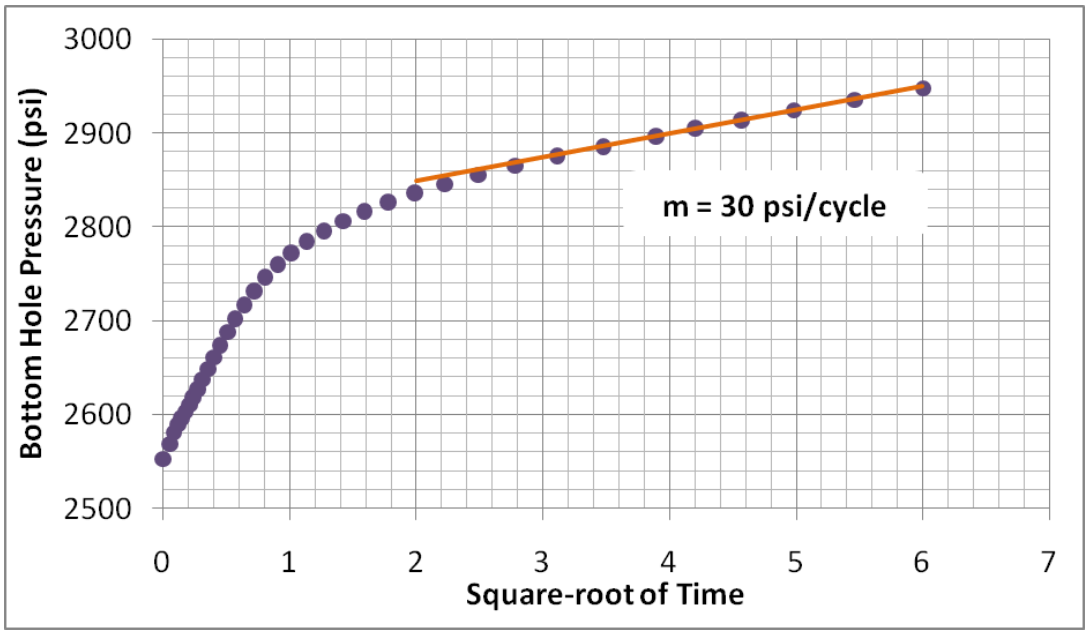

Figure 6.5 – Plot of Linear Horizontal Flow Analysis

The objective of analyzing linear horizontal flow is to determine the permeability in y-direction k_y. Based on Equation 2.36, the permeability can be estimated as follow

$$k_y = \left(8.128 \frac{q\mu B}{mhL\sqrt{\emptyset\mu_o c_t}}\right)^2$$

$$= \left(8.128 \frac{(32392)(0.5)(1.32)}{(30)(37)(4252)\sqrt{(0.26)(0.5)(5.2\times10^{-5})}}\right)^2$$

$$k_y = 201\ mD$$

Data needed for above calculation is provided in Table 6.2.

Table 6.2 – Additional Data for ILF Analysis

Parameter	Value	Unit
B_o	1.32	RB/STB
L	4252	ft
q_o	32393	BOPD
μ_o	0.5	cp
h	37	ft
Φ	0.26	fraction
c_t	5.2×10^{-5}	1/psi

Two flow regimes have been identified, and then both vertical and horizontal permeability is finally determined. The vertical permeability calculated is around 8.2 mD which is much lower than the permeability in y-direction (201 mD). This low k_v/k_h ratio means that the fluid is easier to flow in horizontal direction. Since Garn formation in G-segment has relatively thin layer with respectable wide area, so horizontal permeability play an important role in the production. It might justify that horizontal well in this area is an appropriate technique reinforced by several others considerations.

6.3 Pressure Derivative Analysis Using Software

In order to confirm previous analysis of pressure versus time, then pressure derivative analysis is the next important method to conduct. Combination of both analyses is a powerful technique to identify the flow regimes in horizontal well testing. As mention in theoretical part in Chapter 2.4, vertical radial flow presents as zero slope at the first stabilization in pressure derivative plot. It is continued by 0.5 slope of linear horizontal flow.

Figure 6.6 is a plot of pressure derivative versus time in log-log scale of well E-4AH. The first radial flow represents by orange line with zero slope, and intermediate-time flow is marked by green line with 0.5 slope. As can be seen in the derivative plot, horizontal radial flow regime does not exist. It should be formed after linear horizontal flow regime with slope equal to zero. With standard well testing schedule, this flow regime is rarely appeared; again this is one of complexity in horizontal well testing.

Appendix B provides pressure versus time plots of vertical radial flow and linear horizontal flow analysis using F.A.S.T Welltest™ software. The straight-lines from those plots in Appendix B exactly represent the zero and 0.5 slopes in above figure (derivative pressure plot). This is the main advantages of using the software that user can easily interpret the pressure response by connecting different methods of analysis.

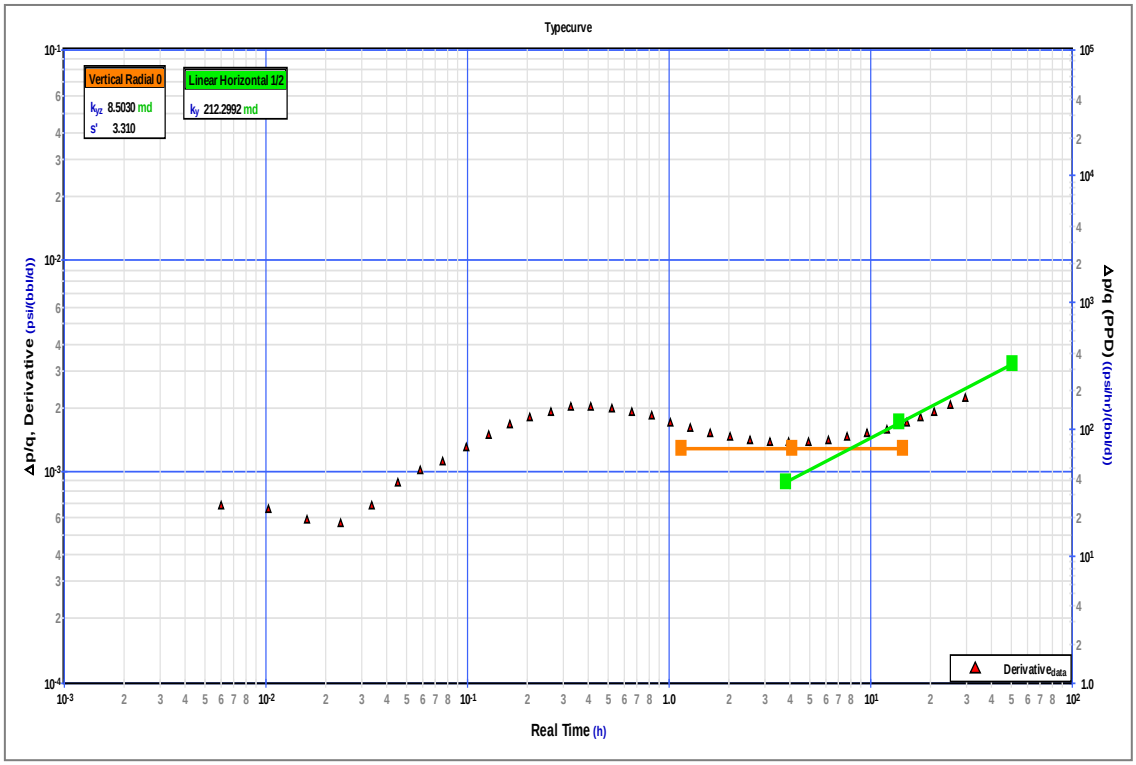

Figure 6.6 – Derivative Pressure Plot of E-4AH Well Test

Table 6.3 provides permeabilities in vertical and y-directions from actual data in model and from pressure transient analysis. All the analyses give sufficient results, especially vertical permeability that deviates only 3.4% from the actual data from reservoir model.

As the first study, comparing the analysis results with the actual data from reservoir model guides the process of a proper interpretation. After acceptable results are obtained, then it clearly gives a good indication for having such the same well testing in the field for real. The real well testing data may use to have an advanced history matching in reservoir model; or generated well test data can still be used to make more sensitivities or forecasts by changing variety parameters in the model itself.

Table 6.3 – Permeability Comparison of Well E-4AH

Reservoir Properties	Data from Reservoir Model	Well Test Result	
		Manual Analysis	Software Analysis
Vertical Permeability, k_{vy} (mD)	8.8	8.2	8.5
Horizontal Permeability, k_y (mD)	253	201	212

CHAPTER 7
CONCLUSION AND RECOMMENDATION

This study is proposed to discuss about pressure transient analysis in Norne field using generated data from simulation. Several wells from different segments were chosen to conduct particular tests and several parameters were obtained. Furthermore, the summaries and conclusions that can be got from this study are discussed in the following sub-chapter. Some recommendations are also proposed to give a better understanding in the future.

7.1 Conclusion

- In reservoir simulation, Local Grid Refinement (LGR) near the wellbore is an important procedure to generate sufficient pressure transient data. It was indicated by the significant differences of pressure responses at Well D-1H from the original reservoir model (Base case) and the refined reservoir models (Case 1, 2, and 3) of Norne field.

- Impact of LGR Area Extension:
    - LGR at Well D-1H should be only applied to a radius of 3950 ft. By exceeding this radius, it generated no pressure deviation between Case 1 and Case 2 which means that LGR might not give any more impact.
    - More accurate permeability calculation was obtained from wider LGR area (Case 2) by giving 6.5% permeability deviation from Case 1 due to considerable pressure deviation after 20 hours of the test. It was the period when the permeability analysis is mainly concerned.
    - There was no difference in storage capacity estimation between Case 1 and Case 2 because of negligible pressure deviation at early time of the test (first 20 hours).

- Impact of LGR Factor Increase:
    - Finer grid is really sensitive at early time of well testing near the wellbore and LGR increment should be stopped when no more pressure difference produced.
    - Finer grid at well D-1H (Case 3) gave more accurate pressure response to a radius of 2040 ft. More than this distance, Case 1 produced the same value with shorter time in simulation.
    - Case 3 had smaller storage capacity as the impact of having finer cells. Its pressure response slightly deviated from Case 1 at the time less than 40 hours. This was the period when the storage capacity calculation is mainly analyzed.
    - Starting from 40 hours of the tests, both Case 1 and Case 3 were getting converges that means permeability calculation is similar, approximately 170 mD.

- Several methods are applicable in pressure transient analysis to determine permeability. Permeability estimation from interference test of well E-3H diverged only 2.4% from buildup test analysis (around 202.5 mD).

- Well E-1H (D-Segment) is surely located in different segment or reservoir properties from well E-2H and E-3H (E-Segment) based on pressure and production trend. The evidences are as follows:
    - Well E-1H had an increasing trend of pressure during production period while the other two wells were decreasing.
    - During shut-in period of well E-3H, production of E-2H was increasing which indicated that fluid in E-segment was concentrated to flow through E-2H. Otherwise, E-1H kept decreasing as the continuation of well production decline profile.

- Based on pressure drop analysis of interference test at well E-3H, it indicated that there is still a communication between D-Segment and E-Segment and the fault which separates them is not fully-sealed. Well E-1H is located across the fault and has greater distance than E-2H, but it still affected the pressure drop in E-3H.

- During transient well testing at horizontal well E-4AH, two identified flow regimes were Vertical Radial flow and Linear Horizontal flow. Horizontal radial flow regime did not exist due to the complexity of well testing in horizontal well.

- Pressure transient analysis of horizontal well E-4AH estimated vertical permeability (8.2 mD) and permeability in y-direction (201 mD). This low k_v/k_h ratio matches the completion strategy (horizontal well) in G-segment which has relatively thin layer of Garn formation with respectable wide area.

7.2 Recommendation

- LGR should be also applied at near-boundary in reservoir model, so then generated well test data can be better analyzed as pressure transient analysis of late time period, if it presents.

- As a comparison to the other types of well tests, permeability determination from drawdown test is good to be conducted.

- Analyzing different type of multiple-well testing (pulse test) will give more information in characterizing the communication between wells or segments in the reservoir.

- Since most of the wells in Norne field are horizontal, so it is a good opportunity to have more analysis and understanding of transient well testing in horizontal well with various type of tests.

REFERENCES

1. **Kamal, Medhat M.** *Transient Well Testing, Monograph Volume 23.* Richardson, TX : Society of Petroleum Engineers, 2009.
2. **Kamal, M. M., Fryder, D. G. and Murray, M. A.** *Use of Transient Testing in Reservoir Management*. SPE-28002-PA, 1995.
3. **Fekete Associates Inc.** FAST WellTest Help Guide. 2010.
4. **Chaudhry, Amanat U.** *Oil Well Testing Handbook.* USA : Elsevier Inc., 2004.
5. **Abdassah, Doddy.** *Production Well Test and Pressure Analysis.* Bandung : Yayasan IATMI, 2005.
6. **Matthews, C. S. and Russel, D. G.** *Pressure Buildup and Flow Tests in Wells (Volume 1).* New York : Society of Petroleum Engineers of AIME, 1967.
7. **Ramey, H. J.** *Short-Time Well Test Data Interpretation in the Presence of Skin Effect and Wellbore Storage.* SPE-2336-PA, 1970.
8. **Agarwal, R. G., Al-Hussainy, R. and Ramey, H. J.** *An Investigation of Wellbore Storage and Skin Effect in Unsteady Liquid Flow: I. Analytical Treatment.* SPE-2466-PA, 1970.
9. **Schlumberger.** Introduction to Well Testing: Section 5 Basic Well Test Interpretation. 1998.
10. **Kamal, M. M.** *Use of Pressure Transients to Describe Reservoir Heterogenerity.* JPT: 1060-1070; Trans., AIME, 267, 1979.
11. **Heinemann, Zoltan E.** *Textbook Series, Volume 4: Well Testing.* Leoben : University of Leoben, 2003.
12. **Earlougher, R. C.** *Advances in Well Test Analysis.* Dallas, TX : Society of Petroleum Engineers, 1977.
13. **Bourdet, Dominique.** *Well Test Analysis: The Use of Advanced Interpretation Models.* Amsterdam : Elsevier Science B.V., 2002.
14. **IPT-NTNU.** Integrated Operations in the Petroleum Industry (IO Center). *Norne Field Information: Introduction to the Norne Field.* [Online] [Cited: May 11, 2012.] http://www.ipt.ntnu.no/~norne/wiki/data/media/english/gfi/introduction-to-the-norne-field.pdf.
15. **Statoil.** Annual Reservoir Development, Norne Field. 2004.
16. **Statoil.** Annual Reservoir Development, Norne and Urd Field. 2006.
17. **NPD.** Norwegian Petroleum Directorate. *Norne: Recoverable Reserves.* [Online] [Cited: May 11, 2012.] http://www.npd.no/en/publications/facts/facts-2012/chapter-10/norne/.
18. **Statoil.** Reservoir Geological Update After 6608/10-4. 1995.

19. **Statoil.** Plan for Development and Operation, Reservoir Geology, Support Documentation. 1994.

20. **Statoil.** PL 128 Norne, Reservoir Management Plan. 2001.

21. **IPT-NTNU.** Integrated Operations in the Petroleum Industry (IO Center). *Package 1: E-Segment.* [Online] [Cited: May 22, 2012.] http://www.ipt.ntnu.no/~norne/wiki/data/media/english/norne_field_case_desc.pdf.

22. **Mattax, Calvin C. and Dalton, Robert L.** *Reservoir Simulation (Monograph Volume 13).* Richardson, TX : Society of Petroleum Engineers, 1990.

23. **Schlumberger.** Eclipse Version 2011.1: Reference Manual. 2011.

NOMENCLATURE

Symbol	Description
A	Drainage area of well, ft^2
B ; B_o	Formation volume factor
C	Wellbore storage capacity, bbl/psi
C_D	Dimensionless wellbore storage coefficient
c_t	Total compressibility, psi^{-1}
h	Formation thickness, ft
k	Formation permeability, mD
k_h	Horizontal permeability, mD
k_h	Horizontal permeability, mD
k_v	Vertical permeability, mD
k_x	Permeability in x-direction, mD
k_y	Permeability in y-direction, mD
L	Effective length of horizontal well, ft
m	Slope
Δp	Pressure drop, psi
p	Pressure, psi
p*	Pressure obtained after infinite closed-in time in an infinite reservoir, psi
$p_{1\,hr}$	Pressure read at time equal to 1 hour, psi
p_D	Dimensionless pressure
p_i	Initial reservoir pressure, psi
p_{wf}	Bottom-hole flowing pressure, psi
p_{ws}	Pressure during shut-in, psi
q ; q_o	Oil production rate of well, bbl/day (BOPD)
r_D	Dimensionless radius
r_e	External boundary radius, ft
r_i	Radius of investigation, ft
r_w	Well radius, ft
s	Skin factor, dimensionless
s_w	Mechanical skin
s_z	Pseudo-skin factor, dimensionless
t	Time, hours
t_D	Dimensionless time
t_{DA}	Dimensionless time for type-curve analysis
t_p	Production time prior to shut-in, hour
t_s	Stabilized time, hours
z_w	Vertical location of well, ft
Φ	Porosity, fraction
μ ; μ_o	Oil viscosity, cp

APPENDICES

Appendix A
Horner Plots and Derivative Plots of Base Case, Case 1, Case 2, and Case 3

These plots are as reference of Chapter 4.

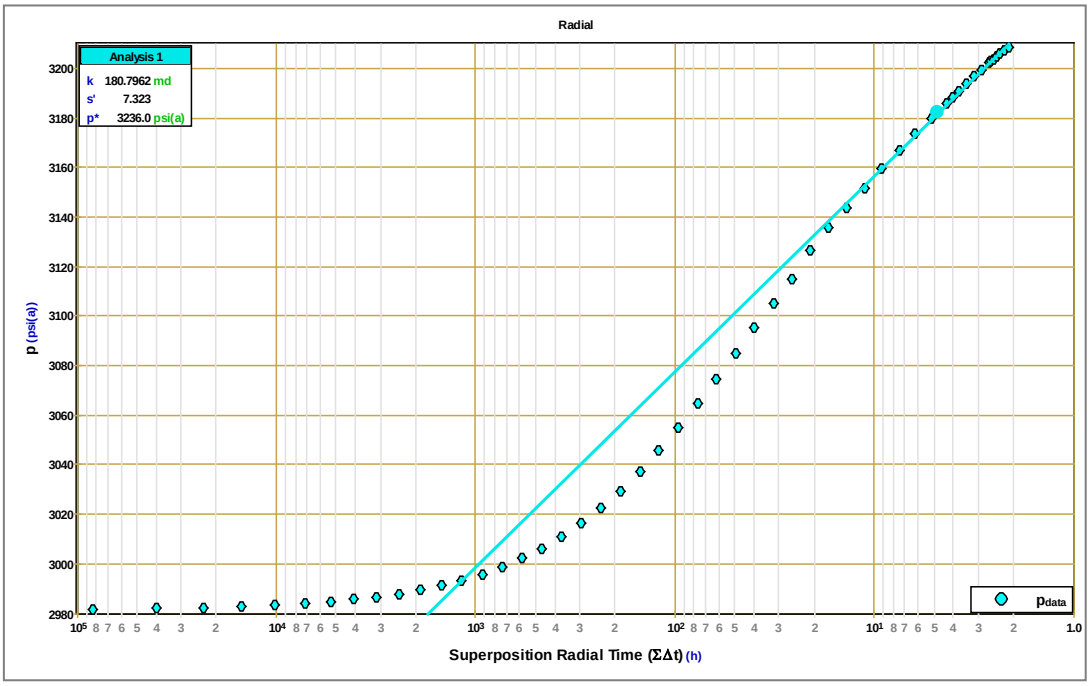

Figure A.1 – Horner Plot of Base Case

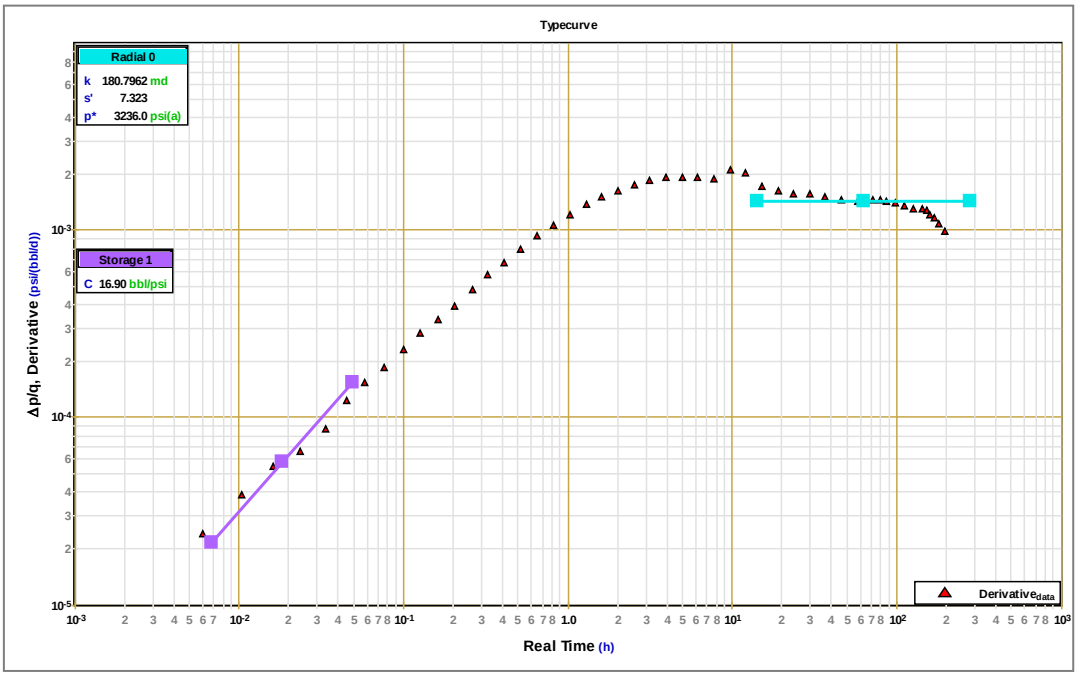

Figure A.2 – Derivative Plot of Base Case

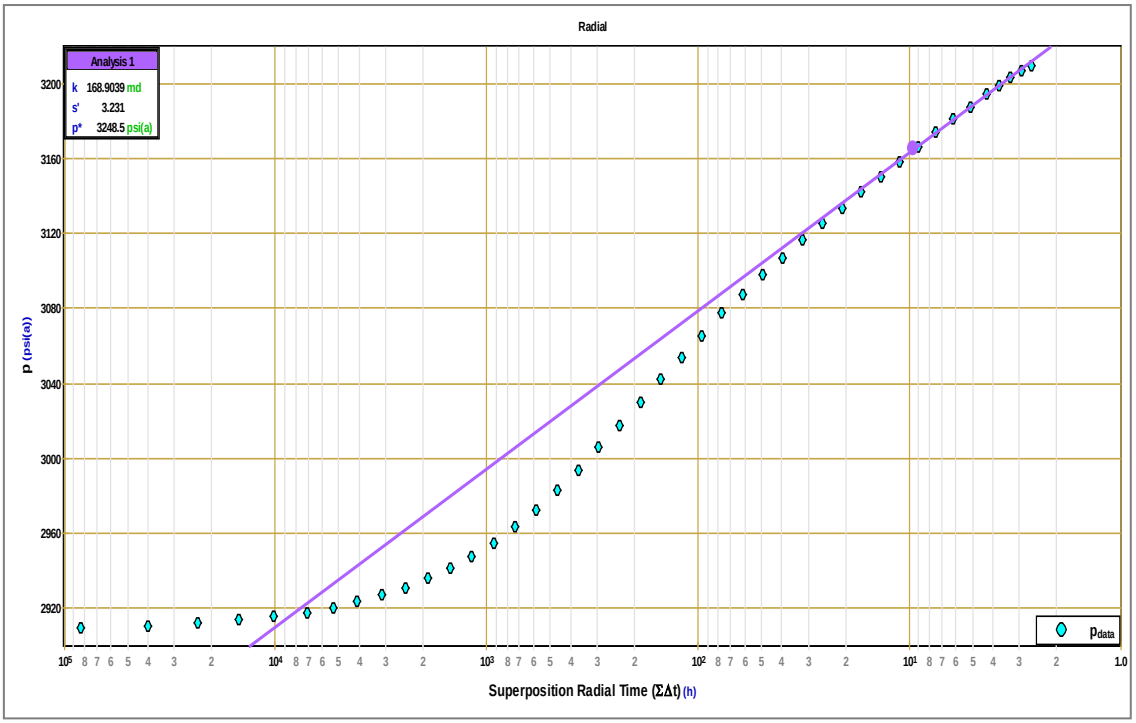

Figure A.3 – Horner Plot of Case 1

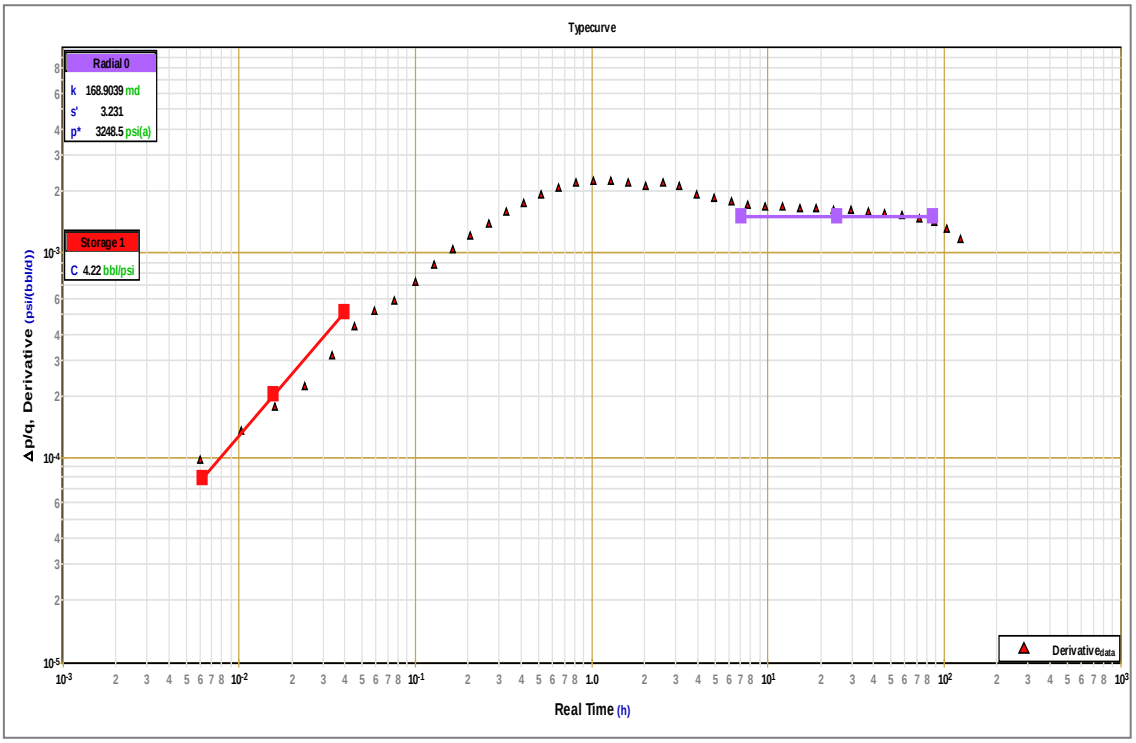

Figure A.4 – Derivative Plot of Case 1

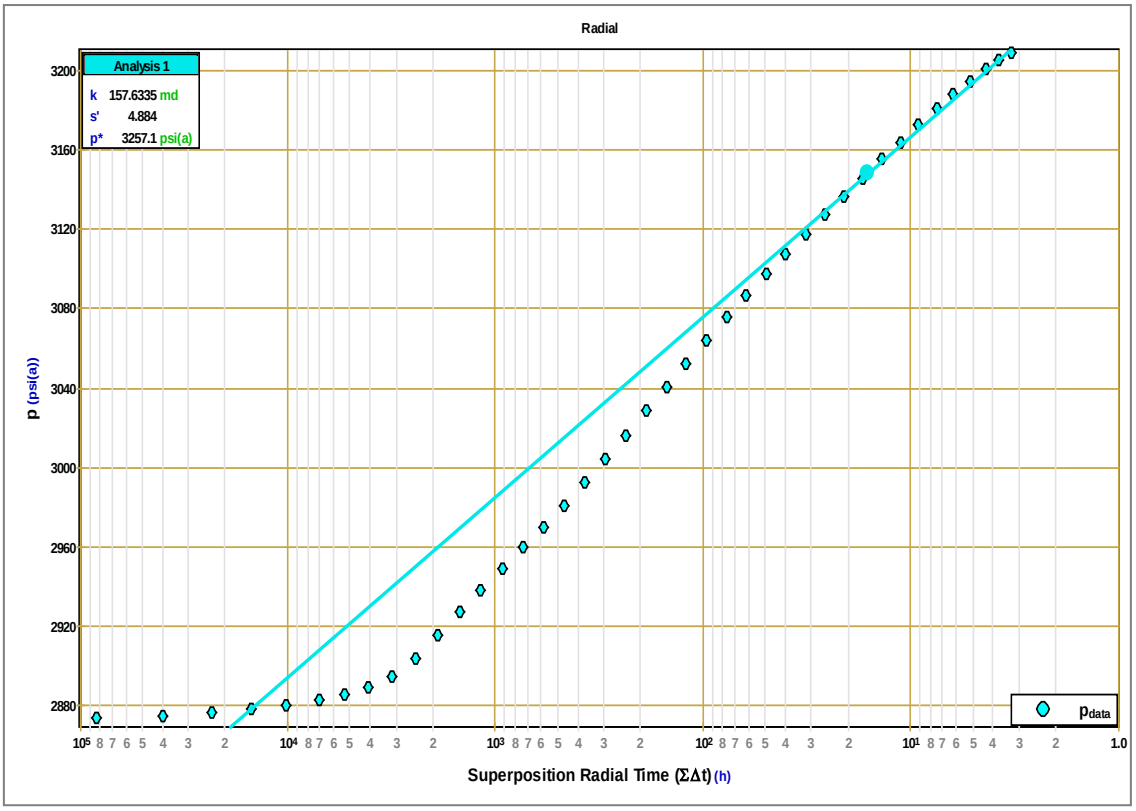

Figure A.5 – Horner Plot of Case 2

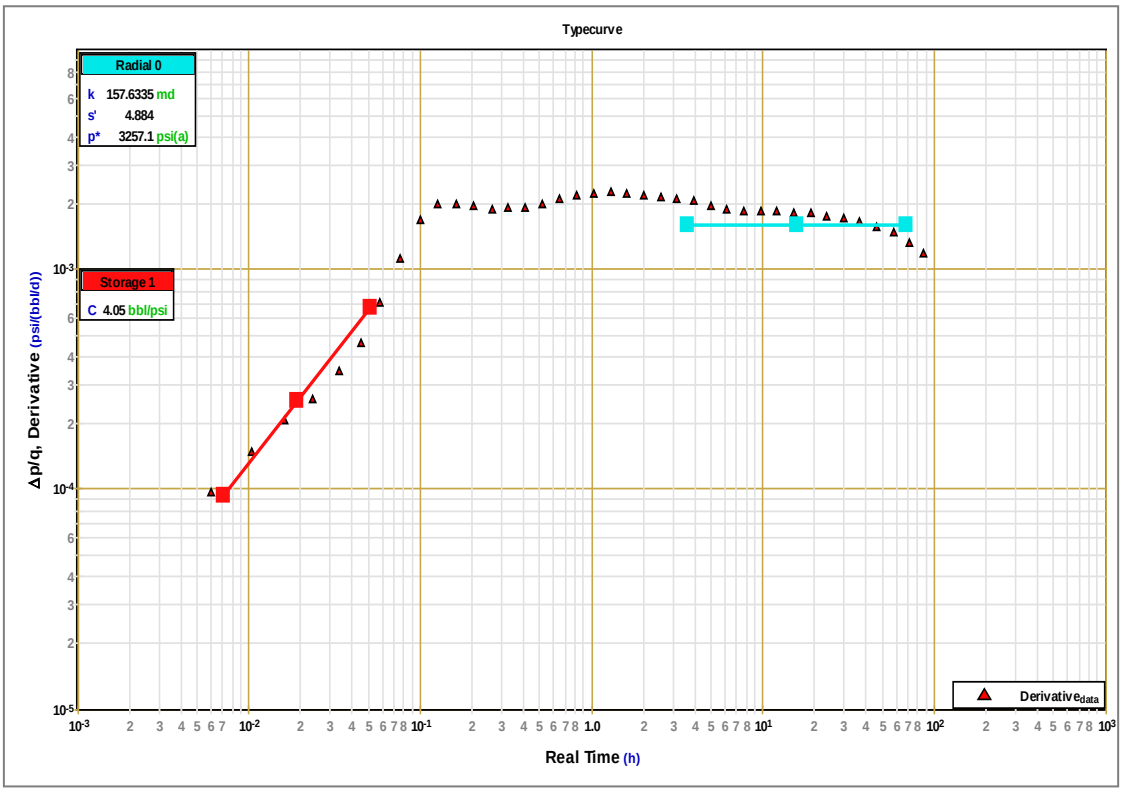

Figure A.6 – Derivative Plot of Case 2

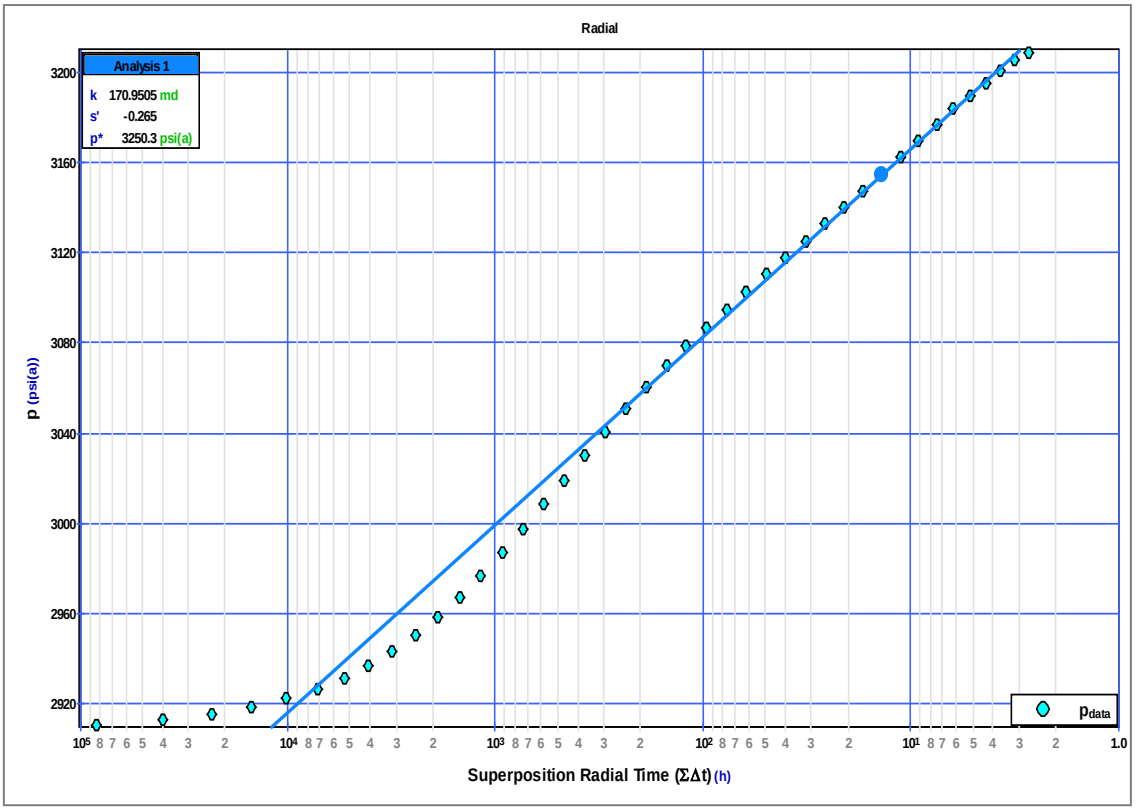

Figure A.7 – Horner Plot of Case 3

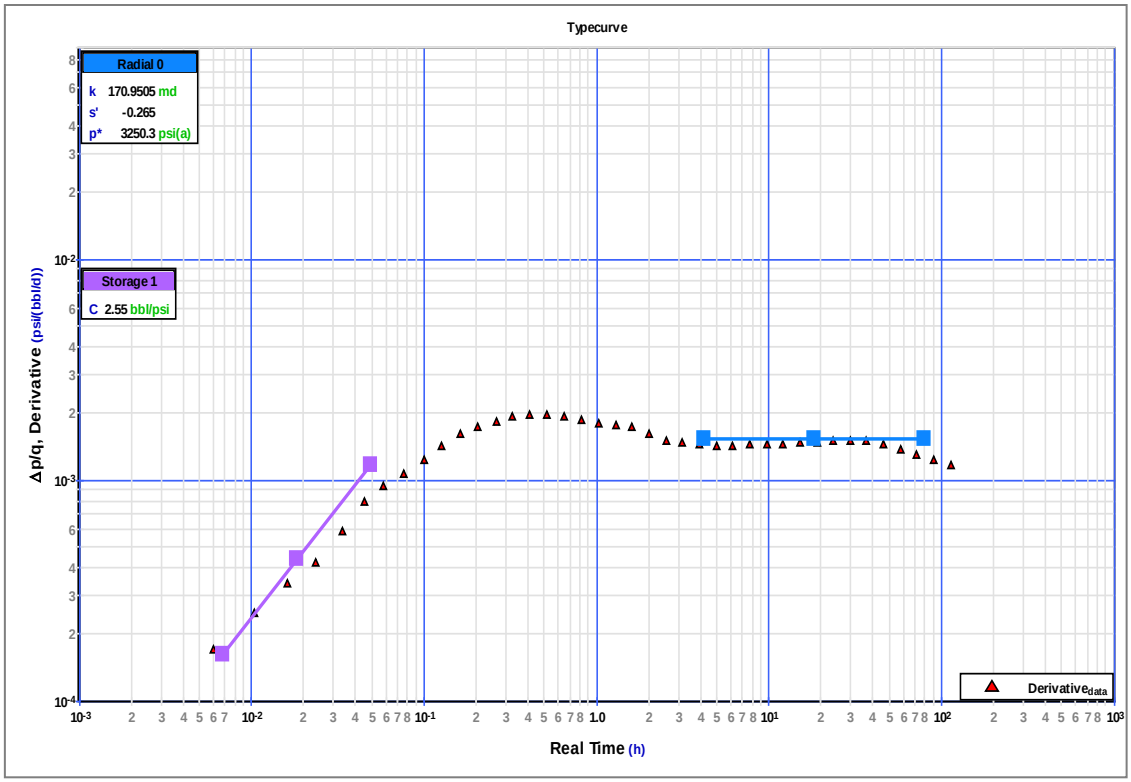

Figure A.8 – Derivative Plot of Case 3

Appendix B
Vertical Radial Flow and Linear Horizontal Flow of Horizontal Well E-4AH

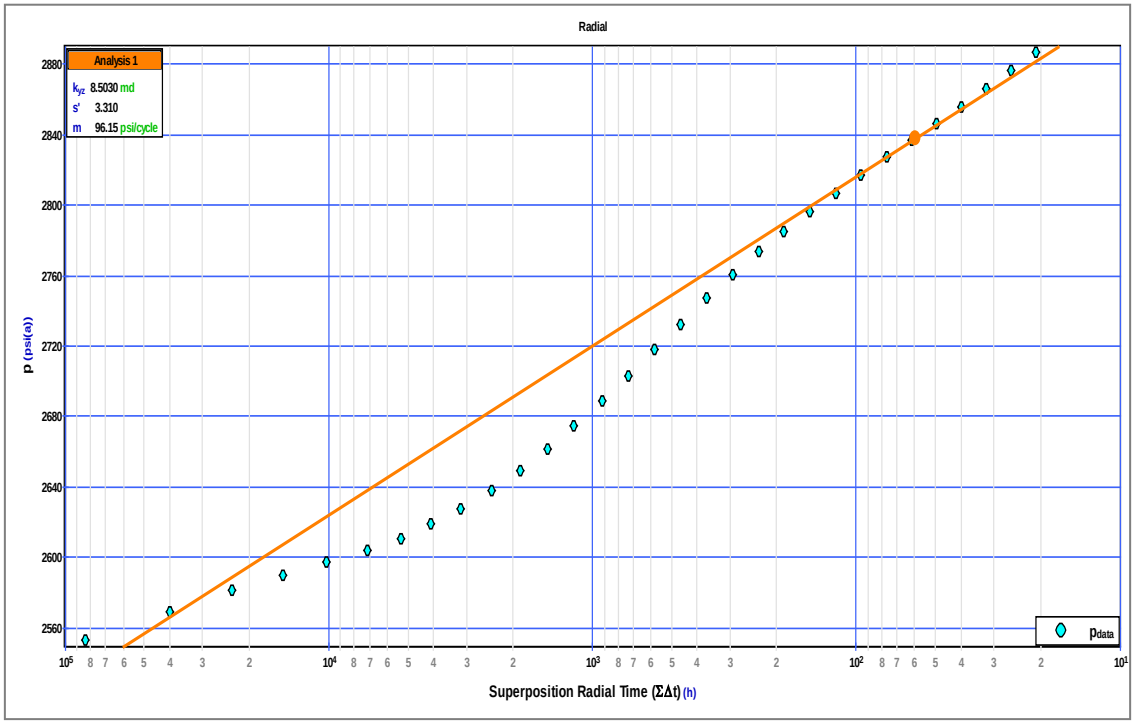

Figure B.1 – Horner Plot of Vertical Radial Flow of Well E-4AH

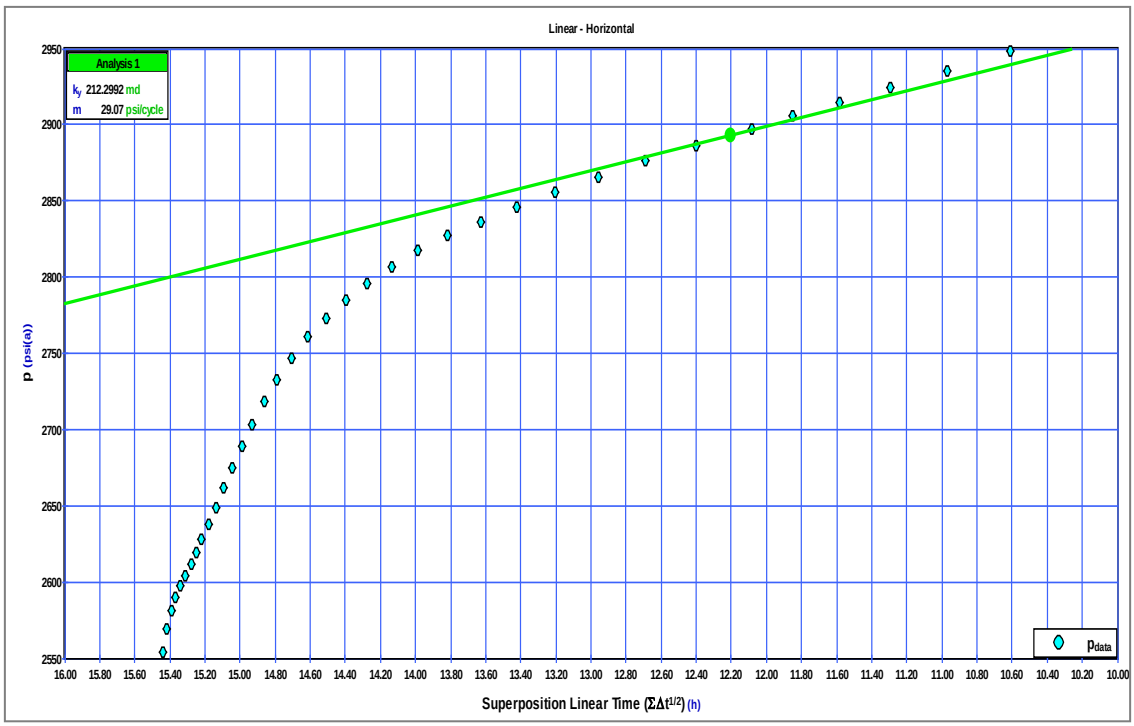

Figure B.2 – Plot of Linear Horizontal Flow of Well E-4AH

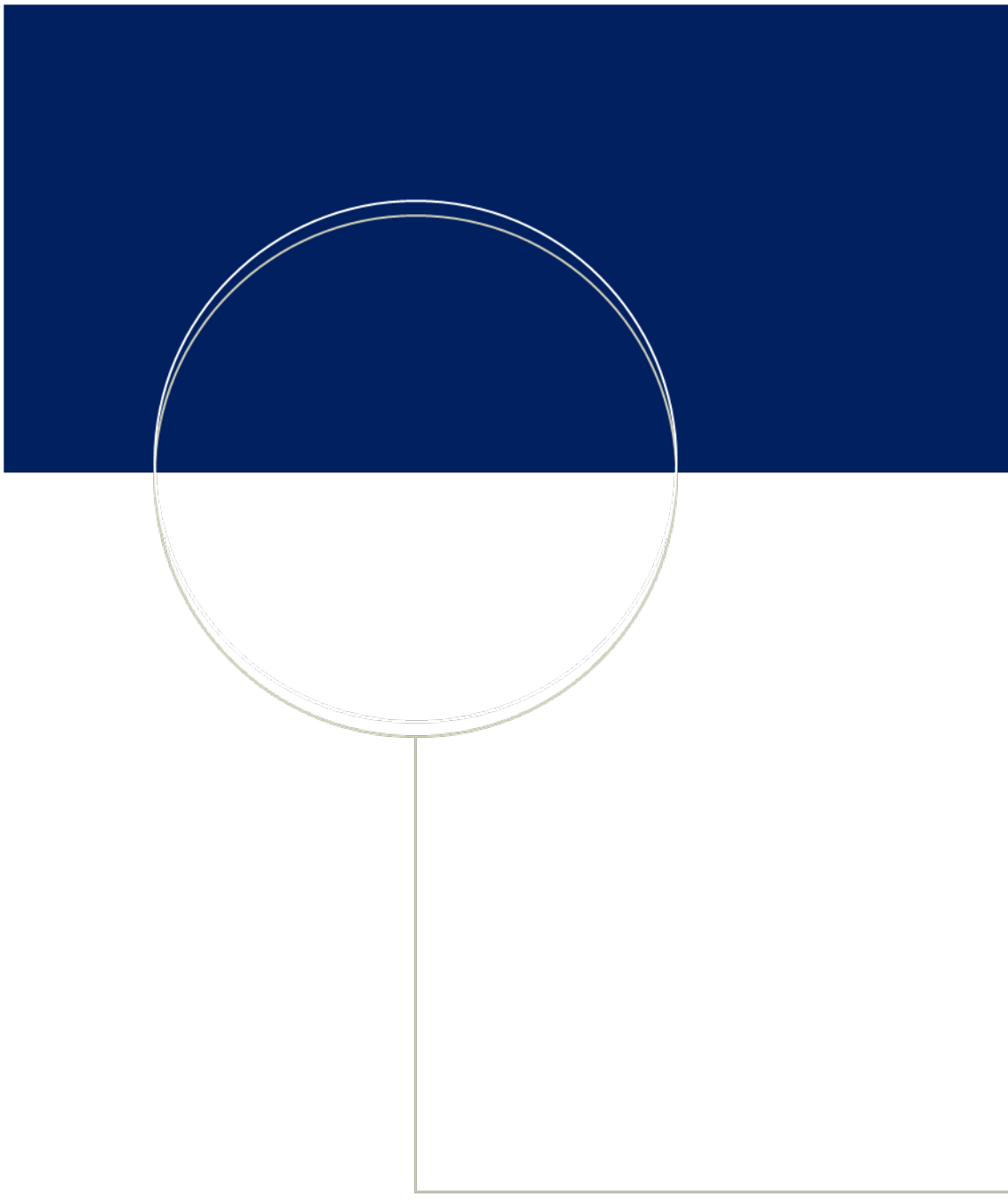

NTNU
Norwegian University of
Science and Technology